



저작자표시-비영리-변경금지 2.0 대한민국

이용자는 아래의 조건을 따르는 경우에 한하여 자유롭게

- 이 저작물을 복제, 배포, 전송, 전시, 공연 및 방송할 수 있습니다.

다음과 같은 조건을 따라야 합니다:



저작자표시. 귀하는 원저작자를 표시하여야 합니다.



비영리. 귀하는 이 저작물을 영리 목적으로 이용할 수 없습니다.



변경금지. 귀하는 이 저작물을 개작, 변형 또는 가공할 수 없습니다.

- 귀하는, 이 저작물의 재이용이나 배포의 경우, 이 저작물에 적용된 이용허락조건을 명확하게 나타내어야 합니다.
- 저작권자로부터 별도의 허가를 받으면 이러한 조건들은 적용되지 않습니다.

저작권법에 따른 이용자의 권리는 위의 내용에 의하여 영향을 받지 않습니다.

이것은 [이용허락규약\(Legal Code\)](#)을 이해하기 쉽게 요약한 것입니다.

[Disclaimer](#)

치의과학박사 학위논문

A critical role of transient receptor
potential canonical 3 in the
peripheral sensory neurons for
mitochondrial reactive oxygen
species – induced itch

미토콘드리아 활성산소종에 의해 유발되는
가려움증에서 감각 신경세포의 transient
receptor potential canonical 3의 역할

2022년 8월

서울대학교 대학원

치의과학과 신경생물학 전공

김 성 아

미토콘드리아 활성산소종에 의해 유발되는
가려움증에서 감각 신경세포의 transient
receptor potential canonical 3의 역할

지도교수 오 석 배

이 논문을 치의과학박사 학위논문으로 제출함

2022년 5월

서울대학교 대학원
치의과학과 신경생물학 전공
김 성 아

김성아의 치의과학박사 학위논문을 인준함

2022년 7월

위 원 장 _____ (인)

부위원장 _____ (인)

위 원 _____ (인)

위 원 _____ (인)

위 원 _____ (인)

Abstract

A critical role of transient receptor potential canonical 3 in the peripheral sensory neurons for mitochondrial reactive oxygen species–induced itch

Seong–Ah Kim

Program in Neuroscience

Department of Dental Science

Graduate School

Seoul National University

Aging increases dry skin–induced chronic itch and causes both mitochondrial dysfunction and an increase of reactive oxygen species (ROS). However, whether mitochondrial ROS (mROS) overproduction contributes to itching has not been explored. Although it is well known that transient receptor potential ankyrin 1 (TRPA1) and transient receptor potential vanilloid 1 (TRPV1) mediate itch, the role of transient receptor potential canonical 3 (TRPC3) in itch is unknown. Therefore, this study aimed to identify a functional link between mROS–induced itch and TRPC3. The results of this study demonstrate that TRPC3 may be relevant to

chronic itch and suggest it may be a potential therapeutic target for this disease.

Antimycin A (AA) can cause mROS overproduction in cells by inhibiting the mitochondrial electron transport chain complex III, thereby inducing mitochondrial malfunction. AA was intradermally injected into mouse cheek skin to determine whether AA-induced mROS caused acute itch. After AA injection, the overproduction of mROS resulted in scratching behavior, which was alleviated by the administration of MitoTEMPO, a mitochondria-selective ROS scavenger or Pyr10, a TRPC3-selective inhibitor. The ROS intensities were increased in both epidermal and dermal tissues. Overproduction of mROS activated small trigeminal ganglion (TG) neurons, and MitoTEMPO or Pyr10 suppressed AA-induced inward currents. mROS-induced currents and scratching behaviors in TRPA1 knockout (KO) mice or TRPV1 KO mice were not different compared to wild type mice. Moreover, mROS-induced currents and scratching behaviors were mediated by TRPC3 but not TRPA1 or TRPV1. TRPC3 was co-expressed with itch-related mediators and receptors in small TG neurons. mROS overproduction also mediated dry skin-induced chronic itch through TRPC3.

In conclusion, mROS elicit acute itch and dry skin-induced chronic itch via TRPC3. This shows that TRPC3 could be a potential target for treating chronic itch and that inhibition of TRPC3 may be effective in relieving chronic itch.

Keyword: mitochondria, reactive oxygen species, TRPC3, itch, dry skin, trigeminal ganglion neuron

Student Number: 2019-36369

* This dissertation includes reproductions from an article published by Seong–Ah Kim, Jun Ho Jang, Wheedong Kim, Pa Reum Lee, Yong Ho Kim, Hue Vang, Kihwan Lee, Seog Bae Oh. Mitochondrial reactive oxygen species elicit acute and chronic itch via transient receptor potential canonical 3 activation in mice. *Neuroscience Bulletin* 38, 373–385 (2022).

<https://doi.org/10.1007/s12264-022-00837-6>

Contents

Abstract	1
Contents	4
List of Figures	5
List of Tables	7
Abbreviation	8
Introduction	11
1. Study Background	11
2. Purpose of Research	17
Materials and Methods	19
Results.....	33
Discussion	59
Conclusion	66
References	67
Abstract in Korean.....	80

List of Figures

Figure 1. An overview of itch transmission from the skin to the spinal cord and brain	26
Figure 2. Crosstalk of the itch and pain pathways in physiological conditions	28
Figure 3. TRP channel family tree.....	29
Figure 4. Molecular mechanism in itch signaling	30
Figure 5. Illustration of mouse behavior pattern to discriminate responses between pain and itch.....	31
Figure 6. AA induces scratching behavior.....	39
Figure 7. Time courses of scratching and wiping.....	40
Figure 8. MitoTEMPO reduces AA–induced scratching behavior	41
Figure 9. Increased mROS in AA–treated skin.....	42
Figure 10. Increased mROS in AA–treated skin and nerve fibers revealed by immunohistochemical analysis	43
Figure 11. Representative trace of AA–induced action potentials	44
Figure 12. Overproduction of mROS by AA treatment depolarizes the membrane potential in small–sized TG neurons	45
Figure 13. Overproduction of mROS by AA treatment evokes inward currents in small–sized TG neurons	46
Figure 14. ROS scavenger inhibits AA–induced currents in small–	

sized TG neurons	47
Figure 15. AA-induced scratching is TRPC3-dependent	48
Figure 16. AA-induced scratching is independent of TRPA1 and TRPV1.....	49
Figure 17. AA-induced inward currents are independent of TRPA1 and TRPV1	50
Figure 18. AA-induced currents are TRPC3-dependent.....	51
Figure 19. Representative expression pattern of itch-related mediators and receptors mRNAs in individual small-sized TG neurons by scRT-PCR	52
Figure 20. TRPC3 co-expresses itch-related mediators and receptors in small-sized TG neurons	54
Figure 21. Experimental designs used for dry skin-induced chronic itch model.....	55
Figure 22. mROS and TRPC3 contribute to dry skin-induced chronic itch	56
Figure 23. Increase of mROS and thickness in epidermis of AEW-treated skin revealed by immunohistochemical analysis.....	57
Figure 24. Increased average intensity of MitoSox-Red and thickness in epidermis	58

List of Tables

Table 1. Similarities and differences between itch and pain	27
Table 2. Primer sequences for scRT-PCR	32
Table 3. Expression of itch-related mediators and receptors including <i>Trpc3</i> , <i>Calca</i> , <i>Trpa1</i> , <i>Trpv1</i> , <i>Mrgpra3</i> , and <i>Mrgprd</i> in individual small-sized TG neurons by scRT-PCR	53

Abbreviations

AA	Antimycin A
ACC	Anterior cingulate cortex
AD	Alzheimer' s disease
AEW	Acetone–ether–water
ALS	Amyotrophic lateral sclerosis
ANOVA	Analysis of variance
ATP	Adenosine triphosphate
ER	Endoplasmic reticulum
Bhlhb5	Helix–loop–helix family member B5
<i>Calca</i>	Calcitonin gene–related peptide (CGRP) encoding gene
CGRP	Calcitonin gene–related peptide
CNS	Central nervous system
DAPI	4 ' , 6–diamidino–2–phenylindole
DIC	Differential interference contrast
DMSO	Dimethyl sulfoxide
dNTP	Deoxynucleotide triphosphate
DRG	Dorsal root ganglion
ER	Endoplasmic reticulum
GABA	Gamma–aminobutyric acid
GAPDH	Glyceraldehyde 3–phosphate dehydrogenase

GPCR	G protein–coupled receptors
GRP	Gastrin–releasing peptide
GRPR	Gastrin–releasing peptide receptor
H1	Histamine receptor 1
HD	Huntington’ s disease
HEK293	Human embryonic kidney 293
HIV	Human immunodeficiency virus
5–HT	Serotonin, 5–hydroxytryptaminHe
IC ₅₀	Half maximal inhibitory concentration
<i>i.d.</i>	Intradermal(ly)
<i>i.p.</i>	Intraperitoneal(ly)
KO	Knockout
mETC	Mitochondrial electron transport chain
MRGPR	Mas–related G protein–coupled receptor
MrgprA3	Mas–related G protein–coupled receptor, member A3
MrgprD	Mas–related G protein–coupled receptor, member D
mROS	Mitochondrial reactive oxygen species
NOX	Nicotinamide adenine dinucleotide phosphate oxidase
PAR2	Protease–activated receptor 2
PBN	Parabrachial nucleus
PBS	Phosphate–buffered saline
PCR	Polymerase chain reaction

PD	Parkinson' s disease
ROS	Reactive oxygen species
SEM	Standard Error of the mean
scRT-PCR	Single-cell reverse transcription polymerase chain reaction
S1	Primary somatosensory cortex
S2	Secondary somatosensory cortex
TG	Trigeminal ganglion
TLR3	Toll-like receptor3
TRP	Transient receptor potential
TRPA	Transient receptor potential ankyrin
TRPA1	Transient receptor potential ankyrin 1
TRPC	Transient receptor potential canonical
TRPC3-7	Transient receptor potential canonical 3-7
TRPM	Transient receptor potential melastatin
TRPM2/8	Transient receptor potential melastatin 2/8
TRPML	Transient receptor potential mucolipin
TRPP	Transient receptor potential polycystin
TRPV	Transient receptor potential vanilloid
TRPV1-4	Transient receptor potential vanilloid 1-4

Introduction

1. Study Background

Itch (or Pruritus)

Nocifensive behaviors, which guard against harmful stimuli, are important for survival. One example of a nocifensive behavior is scratching. To achieve this, endogenous/exogenous pruritogens activate their receptors on the nerve endings of unmyelinated C and myelinated A δ fibers, which then activate second-order neurons in the spinal dorsal horn [1]. After the itch signal is transmitted to the brain, scratching is triggered by itch perception. Itch pathogenesis is broadly categorized into histaminergic and non-histaminergic pathways (**Figure 1**). The histaminergic itch pathway involves histamine secreted by mast cells and transmits acute itch [2–4]. By contrast, the non-histaminergic itch is mediated through nerves expressing various receptors stimulated by pruritogens other than histamine.

Typically, acute itch lasts less than six weeks and causes transient scratching (e.g., an insect bite-induced itch). Although acute itch is regarded as a defense mechanism to protect the body from allergens, in some cases, it can become chronic itch, which lasts longer than six weeks [5]. Chronic itch produces inflammatory skin diseases such as atopic dermatitis, eczema, and psoriasis [6] and is also related to systemic diseases such as diabetes, shingles, liver disease, cancer, autoimmune diseases, and neurological disorders [7, 8].

There are two major itch-transmitting receptor families: GPCRs

and TRP channels. Itch-related GPCRs, which include histamine receptors and MRGPRs, trigger G-protein coupled signaling cascades that mediate the gating of TRP channels [9, 10]. Among the TRP channels, the two typical itch-related channels are TRPA1 and TRPV1. It is well known that TRPA1 plays a crucial role in non-histaminergic itch [10], while TRPV1 is involved in histaminergic itch [11].

Both TRPA1 and TRPV1 are also essential sensors and mediators of pain signals [12–14]. Although itch and pain are distinct sensations, there are also similarities between them (**Table 1**). For example, itch and pain sensations are transmitted through primary sensory neurons, whose cell bodies are located in the DRG or TG [15]. Because itch and pain share many receptors and mediators, itch-sensing neurons are sensitive to pain stimuli. As illustrated in **Figure 2**, in two populations (nociceptors/pruriceptors) of primary sensory neurons responding to pain and itch, respectively, pruriceptor (itch-responsive population) is a very small specific proportion within nociceptors (pain-responsive population).

Several types of pruriceptors express H1, MRGPRs, TRPA1, TRPV1, PAR2, TLR3, and TLR7. Further, there are also several itch-related neuropeptides, such as GRP, CGRP, and substance P. When GRP is released, it activates the itch-specific GRP receptor, GRPR in the spinal cord [16]. The GRPR is not dependent on the histaminergic pathway [17] and GRPR⁺ neurons selectively respond to itch signals but not pain signals [18]. This itch signal can be blocked by Bhlhb5 interneurons, which suppress GRPR⁺ neurons with glycine and GABA [19]. After itch signals enter the spinal cord, they move along the spinothalamic pathway until they reach the thalamus and PBN in the brain. Itch perception is controlled by S1, S2, insula

and ACC [20–22]. When repeated scratching occurs in response to a perceived itch, eventually, the skin barrier becomes impaired and loses moisture. This then intensifies the itch sensation, initiating the 'itch–scratch cycle', which results in skin damage and repetitive itching.

Mitochondrial reactive oxygen species

Mitochondria are the powerhouses of most eukaryotic organisms: they convert oxygen and nutrients into ATP energy and function in cellular metabolic homeostasis, immunity, differentiation, apoptosis, and aging. In addition, mitochondria are the main (up to 90%) producers of intracellular ROS [23], although ROS can also be generated by NOXs, ER, peroxisomes, and phagosomes [24].

ROS are chemical species that include superoxide anion, hydrogen peroxide, and hydroxyl radical derived from molecular oxygen. For normal physiological function, cells regulate the level of ROS, which serve as cell signaling or toxic molecules for normal and abnormal biological processes, respectively. ROS also play a very central role in maintaining the redox balance [25]. Some cellular processes, such as proliferation and differentiation, require low levels of ROS generation [26, 27]. However, elevated ROS levels are characterized by oxidative stress and are related to diseases such as diabetes, inflammatory disease, ischemia–related diseases, cancer, and neurodegenerative disorders [28, 29]. In particular, the CNS is sensitive to oxidative stress because of its high oxygen consumption. Thus, oxidative stress contributes to neurodegenerative diseases such as AD, PD, HD, and ALS [30] .

mROS refers to ROS that originates from mitochondria. Recent studies have suggested that mROS may be involved in cellular

signaling [31]. However, most of the mROS generated by the single-electron reduction of oxygen during the process of oxidative phosphorylation are removed by multiple antioxidant enzymes such as superoxide dismutase, catalase, glutathione peroxidase, and glutathione reductase. Together, these form the mROS scavenging system and function to balance mROS production and elimination [32].

During pathological conditions, mitochondrial dysfunction or damage is often characterized by the overproduction of mROS. This happens either as a result of genetic defects [33] or through the cell damage that occurs in diseases such as cancer and neurodegenerative disease [34, 35]. Mitochondrial dysfunction can also result from the mETC due to an imbalance between cellular oxidant and antioxidant systems [36]. Moreover, it has recently been reported that mitochondrial dysfunction is linked to sensory abnormalities such as nociceptor hyperexcitability [37–39] and that malfunctioning mitochondria are an important cause of the painful peripheral neuropathies resulting from genetic defects, diabetes, or chemotherapy for cancer and HIV [40].

Antimycin A

AA, which is used as a mETC complex III inhibitor, causes ROS production by inhibiting cellular respiration, specifically oxidative phosphorylation. Over time, this persistent increase in ROS levels would likely cause oxidative damage in cells [41]. Furthermore, AA can also hinder cell growth by promoting oxidative stress-mediated apoptosis [42].

It has been shown that intrathecal AA injection induces mechanical hyperalgesia in normal mice in a dose-dependent manner, suggesting a critical role for mROS in pain processing [43].

Besides, inhibition of mETC complex III by AA also activates nociceptive vagal sensory nerves. Nociceptive neuronal activation is diminished by genetic deletion of TRPA1 or TRPV1, as well as inhibition of TRPA1 or TRPV1 [37]. Conversely, ID injection of antimycin attenuates vincristine- or streptozotocin-induced mechanical pain in a dose-dependent manner [44]. However, it has not yet been explored whether mitochondrial dysfunction and the resulting mROS overproduction contribute to an itch sensation.

Transient receptor potential ion channel

Recent advances in itch research have found that TRP channels are crucial players in chronic itch. TRP channels can convert nociceptive/pruritogenic stimuli into electrical signals that pain/itch afferent pathways transmit into the CNS. Moreover, the expression of TRP channels on the skin and in the DRG/TG is directly associated with itch detection.

It is well appreciated that both pain-sensitive and itch-initiating neurons are predominantly small-diameter, unmyelinated C-fiber neurons located in sensory ganglia [45]. Although pain and itch are distinct sensory modalities, they also share many overlapping mediators and receptors in primary sensory neurons [46-48]. Various itch mediators open specific pain/itch-related TRP channels, and depolarize the membrane potential of neurons to transmit signals. However, distinguished subsets of sensory neurons and the spinal ascending tract are involved in transducing pain and itch stimuli [16, 47, 49]. In addition, the excitation of pain-responding sensory neurons can attenuate a scratching response, indicating a connection between the pain- and itch- signaling pathways [50, 51].

TRP channels are a large family of ion channels that are

expressed on the cell membrane and function as non-selective cation channels. TRP channels have six transmembrane helical segments (S1–S6), and their variable amino ($-\text{NH}_2$) and carboxyl ($-\text{COOH}$) terminals are in the cytosol. The pore of the TRP channel is formed by S5 and S6. Various cations, including Na^+ , K^+ , Ca^{2+} , and Mg^{2+} , move through the pore. There are six subfamilies of TRP channels, and of these, TRPC, TRPV, TRPM, TRPA, TRPP, and TRPML are present in mammals (**Figure 3**). TRP channels can be classified into the following two groups: Group 1 (based on high similarity with TRP channels in *Drosophila*): TRPC, TRPV, TRPM, and TRPA; Group 2 (based on low similarity with TRP channels in *Drosophila*): TRPP and TRPML. In addition to their expression in the DRG and TG, TRP channels are ubiquitously expressed in many cell types and tissues, including the brain, pancreas, intestine, and bone. Other than pain and itch, TRP channels are responsible for mediating various sensations such as mechanical stimuli, temperature, and pressure [12, 14, 52–56]. Of the TRP channels, TRPV1, TRPA1, TRPV3, TRPV4, TRPC3, TRPC4, TRPC5, TRPM2, and TRPM8 are sensitive to pain and related to an itching sensation [10, 56–58]. Moreover, TRPV1 and TRPA1 mediate histamine-dependent and histamine-independent itch, respectively [59].

As shown in **Figure 4**, the molecular mechanism of itch signaling is initiated when histamine/chloroquine activate H1/MrgprA3, which couple with TRPV1/A1, respectively, to generate action potentials. Hydrogen peroxide (H_2O_2) may also induce itch by directly activating TRPA1, and ROS can induce itch by directly activating both TRPA1 and TRPV1 [60]. TRPC3 is another ROS-sensitive channel [61–63]. Recently, TRPC was shown to be expressed in MrgprD⁺ non-peptidergic nociceptive neurons, and MrgprD was found to be a

mediator for β -alanine-mediated itch sensation [64]. In another study, Than et al. used the TRPC3 inhibitor, Pyr3 to suppress chloroquine-dependent neural excitability [65], suggesting a function for TRPC3 in itch. Given these previous studies, it is reasonable that TRPC3 is correlated with the itch in addition to TRPA1 and TRPV1 [65].

2. Purpose of Research

Dry skin, mitochondrial dysfunction, and increased ROS can be caused by aging. Age-related physiological changes such as progressive water loss from the skin barrier can also increase dry skin-induced chronic itch. Chronic itch affects approximately 11.5–25.0% of the elderly, particularly those older than 85 years of age [66]. However, anti-histamine treatment shows limited efficacy in most chronic itch types since it only blocks histamine receptors in acute histaminergic itch. Although corticosteroids can be used to treat the inflammation associated with skin diseases, they also have side effects of skin atrophy and hypopigmentation, making them less attractive as therapeutics.

As described earlier, the itch is highly related to pain, and TRPA1 and TRPV1 mediate both itch and pain sensations. It is also known that mROS are involved in pain. However, because the itch-sensing function of TRPC3 is not as well studied as TRPA1/V1, whether there is a relationship between mROS, TRPC3, and itch is still unknown. Additionally, there are sparse itch-related data from TG neurons. Therefore, cell-based studies and a deeper understanding of itch-related molecules are necessary to develop more effective chronic

itch therapies.

In this study, I hypothesized that mROS elicit itch via TRPC3. To investigate whether mROS excites small-sized TG neurons to elicit itch, I used AA to produce mROS endogenously. To demonstrate a functional link between mROS-induced itch and TRPC3, I aimed to generate data supporting the following three statements:

1. AA-generated mROS induce itch.
2. TRPC3 mediates mROS-induced itch.
3. mROS mediate dry skin-induced chronic itch via TRPC3.

Materials and Methods

Animals

The C57BL/6 wild-type and TRPV1 KO mice (5–8 weeks old) were purchased from the Jackson Laboratory. TRPA1 KO mice were obtained from Dr. Justin C. Lee at the Institute for Basic Science (Daejeon, Republic of Korea). Animals were housed in groups of three to five, with free access to water and food under a 12-h light/dark cycle. The protocol of the present study was approved by the Institutional Animal Care and Use Committee at the School of Dentistry, Seoul National University. All efforts were made to minimize animal suffering and to reduce the number of animals used, in accordance with the Guide for the International Association for the Study of Pain.

Chronic itch model

For the cheek model of dry skin-induced chronic itch, the shaved right cheek was treated twice daily (09:00 and 17:00) on five consecutive days with a 1:1 mixture of acetone and ether (15 s) immediately followed by distilled water (30 s), AEW treatment, as described previously [56]. Solutions were gently applied onto the skin with a cotton swab under brief isoflurane (1.5%) anesthesia. Mice were immediately returned to their cage for recovery after each treatment.

Drug preparation and administration

All drugs were from Sigma–Aldrich (St. Louis, MO, USA). For

experiments with AA, 25 mmol/L stock solution was prepared in ethanol and diluted with PBS to final working concentrations. To determine the experimental doses of AA, I referred to the study of Barzegari et al [67]. MitoTEMPO was dissolved in PBS to a final concentration of 100 $\mu\text{mol/L}$, which has been shown to abolish mROS production in various cells including neurons [68]. Pyr10, HC-030031, and AMG-9810 were first dissolved in DMSO to 10 or 100 mmol/L stock solution, and then diluted to final concentrations with PBS. The concentrations of drugs were chosen by previous functional assays of drug efficacy: Pyr10 blocks carbachol-induced Ca^{2+} entry into TRPC3-transfected HEK293 cells with an IC_{50} value of 0.72 $\mu\text{mol/L}$ [69]; HC-030031 antagonizes formalin-evoked Ca^{2+} influx with an IC_{50} of 5.3 $\mu\text{mol/L}$ in TRPA1-expressing HEK293 cells [70]; and AMG-9810 blocks capsaicin-induced rat TRPV1 activation with an IC_{50} of 85.6 nmol/L [71]. Resveratrol at 40 mg/mL was dissolved in DMSO, and then diluted to final concentrations with PBS. Resveratrol improves *in vivo* mitochondrial function and biogenesis in mouse skeletal muscle at a dose of 25–30 mg/kg body weight per day [72]. Corresponding vehicles were prepared in an identical manner without addition of the drugs. All stock solutions were kept at -20°C and diluted to final concentrations immediately before behavioral testing.

Mice were gently restrained by hand without anesthesia for a drug administration. All drugs, except resveratrol, were *i.d.* injected with a 31G insulin needle into the shaved right cheek. The injection volume was 20 μL . *i.p.* injections of resveratrol 100 μL were performed 20 min before each AEW treatment (twice a day for 5 days).

Behavior test

For behavior tests (cheek assay), all tested mice were shaved and then acclimated for 2 days (2 h/day) prior to the testing day. On the day of experiment, naive mice were subjected to drug injection immediately after a 1 h adaptation period. For experiments with the chronic dry skin model, mice were acclimated 1 h before the 2nd AEW treatment on day 5, and then subjected to drug injection in 10 min after AEW treatment. All mice were returned to the observation chambers and video recorded for 30 min immediately after drug injection.

Pain and itch are aversive but are associated with distinct behaviors. Itch or pain behaviors were evaluated as described previously [73]. Briefly, itch behavior was quantified by counting scratching bouts. A scratching bout was defined as lifting a hind limb from the ground and scratching the skin behind the ears and on the back, and then placing the paw back on the ground or grooming it, as described previously [74] (**Figure 5**). Scratching bout consists of a lot of individual scratches which occur so quickly that it is hard to count them separately. For the reason, the number of bouts was counted for scratching behavior test. Evident pain behavior was quantified by counting the number of unilateral wipes of injected site with the fore limb. All behavioral experiments were scored by experimenters blinded to the drug treatments.

Primary culture of trigeminal ganglion neurons

TG neurons were aseptically removed from 5 to 8-week-old mice and digested with collagenase (0.2 mg/mL)/ dispase II (3 mg/mL) for

120 min. Dissociated cells were placed on glass coverslips coated with poly-D-lysine and grown in Neurobasal medium (with 10% fetal bovine serum and 2% B27 supplement) at 37°C with 95% O₂/5% CO₂ for 24 h before experiments. This primary culture excluded the possibility for indirect crosstalk between TG neurons and other cell types.

Whole-cell patch-clamp recordings

Whole-cell voltage- and current-clamp recordings were performed in small (< 25 μm in diameter) TG neurons at room temperature using an EPC10 amplifier with PatchMaster software (HEKA Elektronik, Lambrecht/Pfalz, Germany) or a Multiclamp 700B amplifier with Clampex11.2 software (Axon Instruments, Union City, CA, USA). In voltage-clamp experiments, currents were recorded at a holding potential of -60 mV.

The patch pipettes were pulled from borosilicate capillaries (World Precision Instruments, Sarasota, FL, USA). When filled with pipette solution, the resistance of the pipettes was 4–5 MΩ. The recording chamber (300 μL) was continuously superfused (3–4 mL/min). Series resistance was compensated for (> 80%), and leak subtraction was performed. Data were low-pass-filtered at 2 kHz and sampled at 10 kHz.

The pipette solution contained (in mmol/L): 136 K-gluconate, 10 NaCl, 1 MgCl₂, 5 EGTA, 10 HEPES, 2 Mg-ATP, adjusted to pH 7.3 with KOH. The external solution was composed of (in mmol/L): 140 NaCl, 5 KCl, 2 CaCl₂, 1 MgCl₂, 10 HEPES, 10 glucose, adjusted to pH 7.3 with NaOH.

Skin biopsy procedure

Immediately after sacrifice with isoflurane and cervical dislocation, naive cheek skin was taken using a biopsy punch (2 mm in diameter) and rinsed in PBS for 10 min. After removing residual PBS, the biopsied skin was incubated in MitoSox-Red (50 μ mol/L) (Sigma-Aldrich, St. Louis, MO, USA) for 30 min. The tissue was rinsed again with PBS and fixed in 4% paraformaldehyde in PBS overnight at 4°C.

For AEW-treated skin collection, the same procedure was performed 10 min after the last AEW treatment on day 5. To prepare AA-treated skin, biopsy skin was incubated in AA (50 μ mol/L) for 30 min with following PBS rinse for 10 min. MitoSox-Red (50 μ mol/L) was then applied to the skin for 30 min with following PBS rinse for 10 min. The skin sample was fixed in 4% paraformaldehyde in PBS overnight at 4°C.

Immunostaining

Fixed skin samples were rinsed with PBS and placed in 30% sucrose in 1 \times PBS for at least 3 days. Then, the samples were frozen and cut at 20 μ m in the vertical plane on a vibrating microtome (VT1000 Plus, Leica, IL, USA). The sections were washed 5 times for 10 min each in PBS and immunostained on slides overnight at 4°C with an antibody against β -tubulin III (rabbit anti-TuJ1, 1:500, Sigma-Aldrich, St. Louis, MO, USA), a neuron-specific marker. Following 5 rinses with PBS for 30 min each, the sections were incubated in donkey anti-rabbit FITC-conjugated secondary antibody for 90 min (1:200, Jackson ImmunoResearch, West Grove, PA, USA). The sections were then rinsed again 3 times in PBS for 30 min each and mounted with Vectashield with DAPI (Vector labs, Burlingame, CA,

USA).

Image analysis

Data were acquired on a laser scanning confocal microscope (LSM 700, Carl Zeiss GmbH, Jena, Germany). The targeted skin area including epidermis and dermis was captured with 40× objective. Single-plane and multi-focal z-stack images were acquired for DIC and fluorescence images, respectively. The fluorescence intensity of MitoSox-Red was measured in epidermis and dermis separately using Zen software (Carl Zeiss GmbH, Jena, Germany). Skin sections that included hair shafts and follicles were excluded due to the high fluorescence activity and uneven distribution. The outermost layer of the epidermis consisting of dead cells and DAPI-stained areas that did not have mitochondria were also excluded from data analysis. Average fluorescence intensity from each section was calculated as follows:

$$\text{Average intensity} = \frac{\sum (\text{intensity} \times \text{corresponding pixel numbers})}{\text{(Total pixel numbers)}}$$

Two to four sections were obtained from each mouse for data analysis. The epidermal thickness was measured from DIC images taken at 2–3 random fields per section using Zen software. All sections were stained and imaged together with the same settings.

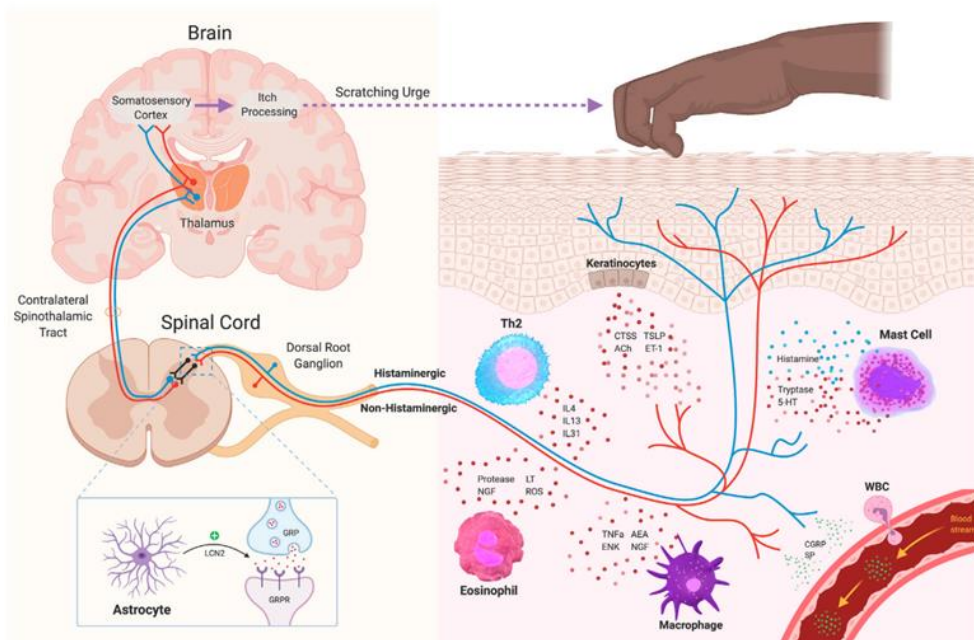
Single-cell reverse transcription polymerase chain reaction

scRT-PCR was performed as previously described [75]. Briefly, the targeted cell was collected using a patch pipette with tip diameter of about 20 μm and put into PCR tube containing reverse transcription

reagents. The reagents were incubated for 10 min at 25°C, 90 min at 50°C, then 5 min at 85°C for cDNA synthesis. The cDNA products were stored at -20°C until further processing. All PCR amplifications were performed with nested primers (Bioneer, South Korea, information listed in **Table 2**). The first round of PCR was performed in 50 μ L of PCR buffer containing 0.2 mmol/L dNTPs (Invitrogen, Carlsbad, CA, USA), 0.2 μ mol/L “outer” primers, 1–3 μ L RT product, and 0.2 μ L platinum Taq DNA polymerase (Invitrogen, Carlsbad, CA, USA). For the second round of amplification, the reaction buffer (50 μ L) contained 0.2 mmol/L dNTPs, 0.2 μ mol/L “inner” primers, 2 μ L products from the first round, and 0.2 μ L platinum Taq DNA polymerase. The PCR products were then displayed on Safe–Pinky stained 1.5% agarose gel. The gels were photographed using a UV digital camera.

Statistical analysis

All data are represented as the mean \pm SEM. These tests were performed using an unpaired *t*-test or one-way ANOVA followed by Tukey’ s *post hoc* test and were analyzed using Prism 5.0 (GraphPad Software, CA, USA). *p* values < 0.05 were considered statistically significant. * *p* < 0.05, ** *p* < 0.01, *** *p* < 0.001.



Sutaria et al. J Am Acad. Dermatol. (2022)

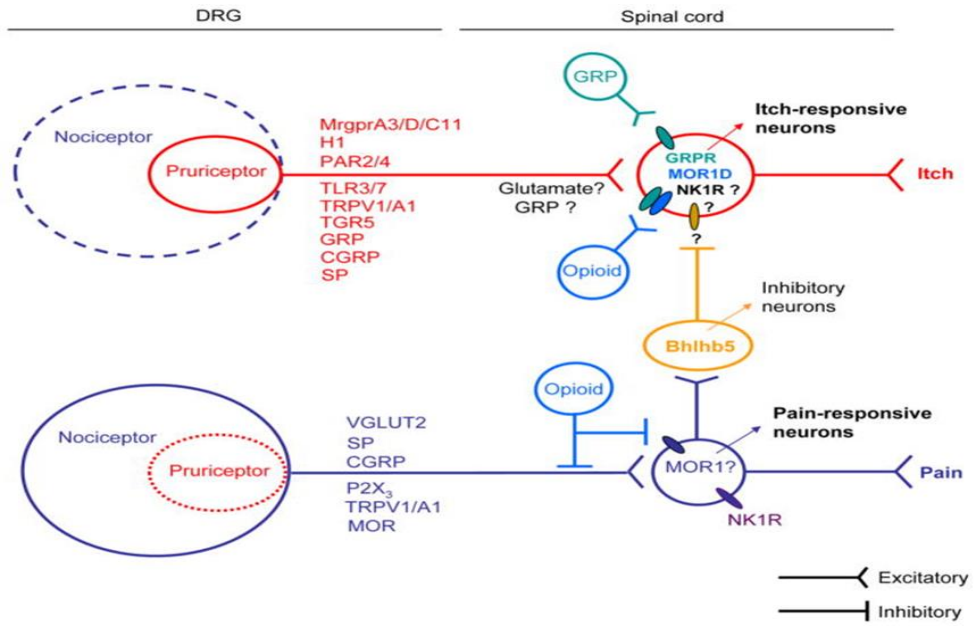
Figure 1. An overview of itch transmission from the skin to the spinal cord and brain.

5-HT (serotonin), Ach (acetylcholine), AEA (anandamide), CGRP, (calcitonin gene-related peptide), CTSS (cathepsin S), ENK (enkephalin), ET-1 (endothelin-1), GRP (gastrin-releasing peptide), GRPR (gastrin-releasing peptide receptor), IL4 (interleukin 4), IL13 (interleukin 13), IL31 (interleukin 31), LCN2 (lipocalin-2), LT (leukotrienes), NGF (nerve growth factor), ROS (reactive oxygen species), SP (substance P), Th2 (Type 2 helper T cell), TNF α (tumor necrosis factor alpha), TSLP (thymic stromal lymphopoietin), WBC (white blood cell)

	Similarities	Differences
Acute states	<p>Both are unpleasant sensations</p> <p>Both are protective in the normal conditions</p> <p>Both are mediated by capsaicin-sensitive C-fibers</p> <p>Both are regulated by proinflammatory mediators (e.g., histamine, 5-HT, ET-1, and PGs)</p> <p>Both employ similar ion channels, such as TRPV1 and TRAP1</p> <p>Both may use glutamate and neuropeptides (SP and CGRP) as neurotransmitters</p>	<p>Itch stimuli evoke scratching while pain stimuli induce withdrawal reflex</p> <p>Itch origins from the skin or mucosal surfaces, while pain origins from almost all body parts</p> <p>Itch is inhibited by painful stimuli</p> <p>Inhibition of pain by analgesic such as morphine can provoke itch</p> <p>Only a small portion of primary nociceptive neurons respond to itch</p> <p>Itch is mediated by MrgA3+ primary sensory neurons and GRPR+ dorsal horn neurons</p>
Chronic states	<p>Both are debilitating conditions in patients and pets</p> <p>Pain stimuli can be perceived as itch sensation in atopic dermatitis</p> <p>Both are enhanced by peripheral sensitization, elicited by inflammatory mediators (e.g., NGF, TNF-α) and TRPA1/V1</p> <p>Both are potentiated by central sensitization, such as loss of inhibitory control and enhanced excitatory synaptic transmission</p> <p>Both are regulated by immune cells and glial cells in the PNS and CNS</p> <p>Both can be reduced by gabapentin, pregabalin, local anesthetics, clonidine, and antidepressants</p>	<p>Itch is mediated by specific cytokines (IL-2, IL-13, or IL-31), while pain is elicited by various cytokines (e.g., IL-1β, IL-6, etc.) and chemokines (e.g., CCL2, CCL5, CXCL1)</p> <p>μ-opioid receptor agonists induce itch while μ-opioid receptor antagonists reduce itch</p> <p>κ-opioid receptor agonists reduce itch while κ-opioid receptor antagonists induce itch</p>

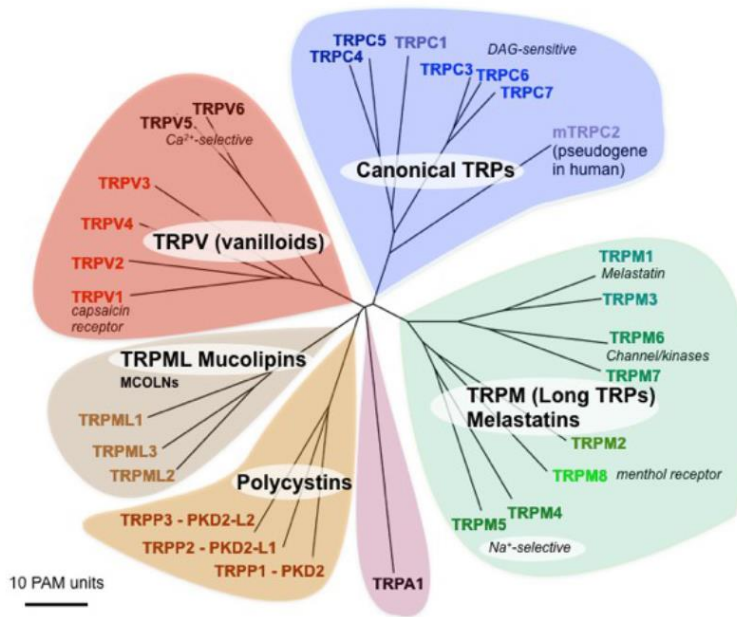
Tong Liu & Ru-Rong Ji, Pflugers Arch (2013)

Table 1. Similarities and differences between itch and pain.



Tong Liu & Ru-Rong Ji, Pflugers Arch (2013)

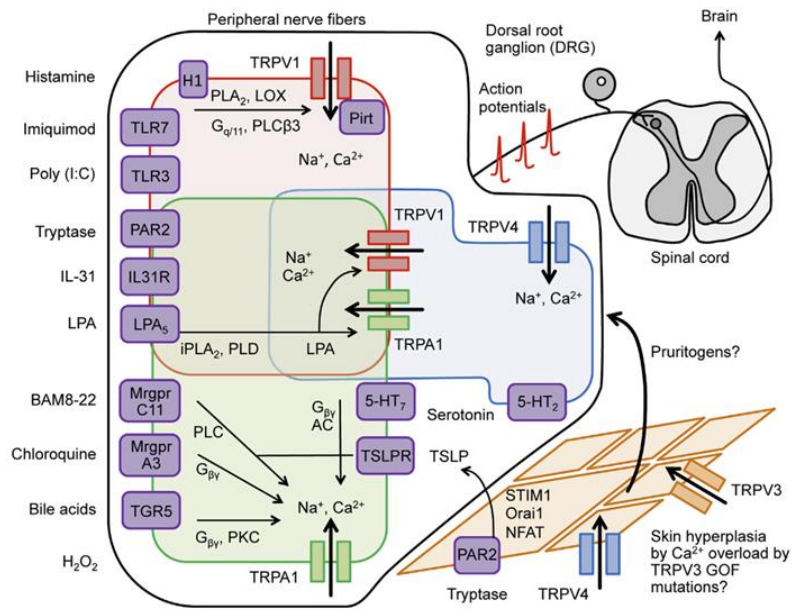
Figure 2. Crosstalk of the itch and pain pathways in physiological conditions.



*Modified from Nature 426: 517–524 (2003)
 by Nathaniel T. Blair et al. IUPHAR/BPS guide to Pharmacology CITE (2022)
 (This is an open access article under the CC BY–SA license.)*

Figure 3. TRP channel family tree.

There are six families of TRPs including TRPA, TRPC, TRPV, TRPM, TRPP, and TRPML in mammals.

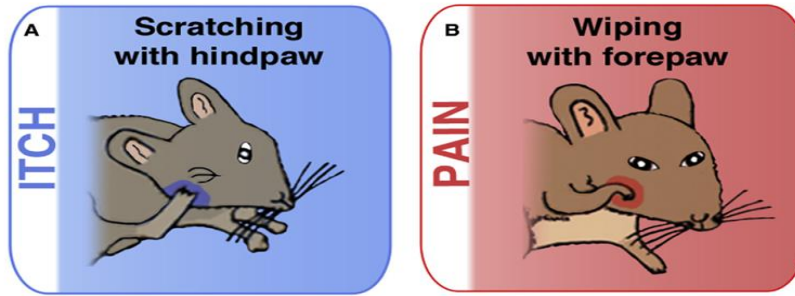


H. Kittaka, M. Tominaga, Allergology International (2017)

(This is an open access article under the CC BY-NC-ND license.)

Figure 4. Molecular mechanism in itch signaling.

Various endogenous and exogenous itch mediators activate their specific receptors. Activation of these receptors couples with TRPA1, TRPV1, and TRPV4 to generate action potentials and then electrical signals are transmitted to the brain via spinal cord.



Kardon et al. Neuron (2014)

(This is an open access article under the CC BY license.)

Figure 5. Illustration of mouse behavior pattern to discriminate responses between pain and itch.

Illustration shows pain-wiping behavior with forepaw and itch-scratching behavior with hindpaw.

Target gene	Outer primer sequences (5'-3')	Inner primer sequences (5'-3')	Product length (bp)	GeneBank accession no.
<i>Trpc3</i>	(For) TCAGCCAACACGATATCAGC (Rev) GGTCAACTGCTGGAACCATT	(For) GAACCCAGTGTGCTGAGAT (Rev) GGTCAACTGCTGGAACCATT	Outer; 420 Inner; 210	NM_019510
<i>Calca</i>	(For) TGGTGCAGGACTATATGCAG (Rev) TATCCCCTTGAGGTTAGCA	(For) GCCCCAGAATGAAGTTACA (Rev) CAACACGATGCACAATAGGC	Outer; 547 Inner; 187	NM_001289444
<i>Trpa1</i>	(For) AGCCACCCGACTTTTAGTT (Rev) GTCATGTGTGATGGGACGAG	(For) AAACCAGGGTTGTTGGAATG (Rev) ATGTGTGATGGGACGAGGAG	Outer; 471 Inner; 219	NM_177781
<i>Trpv1</i>	(For) CATGCTCATTGCTCTCATGG (Rev) AACCAGGGCAAAGTTCTTCC	(For) CATGGGCGAGACTGTCAAC (Rev) CTGGGTCTCGTTGATGATG	Outer; 352 Inner; 248	NM_001001445
<i>Mrgpra3</i>	(For) GGGACATCTTTATCGGAGCA (Rev) ACAGTGGTCAAGTGCAGCAG	(For) GATTGCACCTGGTGTGTTTG (Rev) ATCACGGCTCTGCTTTGTTT	Outer; 483 Inner; 218	NM_153067
<i>Mrgprd</i>	(For) AGGCTCCTTTCATCCCAAGT (Rev) CCATGCTGGGAGAACTTA	(For) GCTCCTTTCATCCCAAGTGA (Rev) TAACCCCTGGACCACACTTC	Outer; 366 Inner; 277	NM_203490
<i>Gapdh</i>	(For) AACAGCAACTCCCACTCTTC (Rev) TGGGTGCAGCGAACTTTAT	(For) ACTCCCACTCTTCCACCTTC (Rev) TGAGGGAGATGCTCAGTGTT	Outer; 329 Inner; 230	NM_008084

Table 2. Primer sequences for scRT-PCR

Results

Overproduction of mROS induces scratching behavior in mice

I first investigated whether ROS specifically derived from mitochondria induced scratching behavior [73]. AA has been widely used to generate mROS overproduction through mitochondrial modulation by inhibiting mETC complex III in a variety of cells including neurons [76, 77].

As shown in **Figure 6**, ID injection of AA (10, 25, 50, and 100 μ mol/L) elicited itch-like scratching behavior for 30 min ($n = 8$ per group) in a dose-dependent manner, similar to the inverted U-shaped dose responses reported with some other pruritogens [78–81]. The response at 50 μ mol/L AA, which was the most effective dose to elicit scratching behavior, started after a 10 min delay, peaked between 10 and 20 min after injection, and then weakened afterward (**Figure 7A**). Interestingly, AA-induced scratching behavior was exclusively itching without wiping behavior which represented a pain response by the forelimb, at least in my tested drug concentration ranges (**Figure 7**), suggesting that overproduction of mROS by AA injection may be related to itch, but not pain signaling, while ethanol (0.4%)–vehicle did not induce noticeable scratching or wiping behavior. AA-induced scratching behavior was markedly suppressed by co-injection with a mitochondria-selective ROS scavenger, MitoTEMPO (100 μ mol/L), compared to the PBS–vehicle group ($p < 0.05$, unpaired t -test, $n = 7$ per group, **Figure 8**). MitoSox–Red, which is a mitochondria specific ROS indicator, was evidently increased both in epidermal and dermal layers of cheek

skin compared to naive tissue (50 $\mu\text{mol/L}$ of AA, $p < 0.01$, unpaired t -test, $n = 5-7$ per group, **Figure 9, 10A, and 10B**). While a strong MitoSox-Red signal was detected in the epidermal layer, ROS expression was comparatively low in the dermal layer after AA-intradermal injection (**Figure 9, 10A, and 10B**). MitoSox-Red co-labeled with β -tubulin III was detected along nerve fibers in the dermis, indicating direct production of mROS from nerve terminals themselves (**Figure 10C**).

Overproduction of mROS activates small-sized TG neurons

I next determined whether mROS evoked by mitochondrial dysfunction activated TG neurons using whole-cell patch clamp recordings. As shown in **Figure 11 and 12A**, the application of AA depolarized the membrane potential in 55.5% ($n = 10$ of 18) of small TG neurons while it was never recorded with vehicle treatment (unpaired t -test, $p < 0.001$, $n = 18$ per group). The majority of neurons (80%, $n = 8$ of 10) generated action potentials with AA application but not vehicle treatment (unpaired t -test, $p < 0.05$, $n = 10$ per group, **Figure 12B**). To address the mechanism of AA-induced depolarization, I tested AA induced currents in small-sized TG neurons at a holding potential of -60 mV, and found that 66.6% ($n = 10$ of 15) of neurons showed such inward currents (**Figure 13**). Then, the AA-induced inward currents were completely prevented in 90% ($n = 9$ of 10) cells by MitoTEMPO (100 $\mu\text{mol/L}$, $p < 0.05$, unpaired t -test, $n = 10-15$ per group, **Figure 13 and 14**). Interestingly, I observed that stepwise inward currents were recorded in all tested AA-responsive neurons; these were not washed out but were prevented by MitoTEMPO, suggesting that

persistent generation of mROS by AA application induced the activation of ion channels and elicited membrane depolarization in small-sized TG neurons.

TRPC3 mediates both mROS-induced scratching behavior and inward currents

To explore whether TRPC3 involved in the modulation of mROS-induced itch, I assessed the effect of Pyr10, a selective inhibitor of TRPC3 channels [69], on AA-induced scratching behavior. As shown in **Figure 15**, co-injection with Pyr10 (1, 10, and 25 $\mu\text{mol/L}$) inhibited the AA (50 $\mu\text{mol/L}$)-induced scratching in a dose-dependent manner. Pyr10 at 10 and 25 $\mu\text{mol/L}$ significantly suppressed AA-induced scratching behavior compared to the vehicle group (0.25% DMSO, $p < 0.05$, one-way ANOVA followed by Tukey's *post hoc* test, $n = 7-9$ per group). In addition, I investigated whether TRPA1 and TRPV1, which were ROS-sensitive and itch-related channels, contributed to AA-induced scratching behavior. The results showed that AA-induced scratching behavior was not affected by co-injection with HC-030031 (100 $\mu\text{mol/L}$ or 1 mmol/L), a selective TRPA1 blocker, or AMG-9810 (100 $\mu\text{mol/L}$), a potent TRPV1 antagonist, compared to the vehicle-treated group (one-way ANOVA followed by Tukey's *post hoc* test, $n = 8-15$ per group, **Figure 16**). AA-induced scratching behaviors in TRPA1 KO and TRPV1 KO mice were comparable with that of the vehicle-treated group (one-way ANOVA followed by Tukey's *post hoc* test, $n = 8-15$ per group, **Figure 16**). I also examined whether AA-induced current was mediated via TRPC3 in small-sized TG neurons. As noted previously, stepwise inward currents were induced by 50 $\mu\text{mol/L}$ AA. I found that AA-induced currents in TRPA1 KO and

TRPV1 KO did not differ from those of wild-type mice in small-sized TG neurons (one-way ANOVA followed by Dunnett's *post hoc* test, $n = 4-12$ per group, **Figure 17**). The IC_{50} of Pyr10 for TRPC3, $1 \mu\text{mol/L}$ [28], decreased the AA-induced inward currents by about half ($50.63 \pm 7.6\%$ for $1 \mu\text{mol/L}$ AA, $p < 0.001$, paired *t*-test, $n = 8$ per group, **Figure 18A and 18B**). When the currents reached a plateau in the presence of AA, co-application of Pyr10 (10 or $25 \mu\text{mol/L}$) almost completely abolished them (**Figure 18C and 18D**). The reversible blockade effects were found at both $10 \mu\text{mol/L}$ ($p < 0.001$, paired *t*-test, $n = 5$ per group) and $25 \mu\text{mol/L}$ ($p < 0.001$, paired *t*-test, $n = 6$ per group) of Pyr10 compared to the vehicle groups (0.1% DMSO, **Figure 18C and 18D**). These results showed that the AA-induced inward current was mediated by TRPC3 but not TRPA1 or TRPV1 in small-sized TG neurons.

TRPC3 is co-expressed with itch-related mediators and receptors in small-sized TG neurons

To determine a functional interaction between well-known itch-related mediators and receptors in nociceptive primary afferent TG neurons, I investigated transcripts corresponding to *Trpc3*, *Calca*, *Trpa1*, *Trpv1*, *Mrgpra3*, and *Mrgprd*, in 34 small-sized TG neurons using scRT-PCR (**Table 3**). The average of cell diameter used scRT-PCR is $18.50 \pm 0.44 \mu\text{m}$ (**Figure 19A**). As shown in **Figure 19B and Table 3**, *Trpc3*, *Trpa1*, and *Trpv1* were detected in 35.2% ($n = 12$ of 34), 32.3% ($n = 11$ of 34), and 23.5% ($n = 8$ of 34) of small-sized TG neurons, respectively. The expression of *Mrgpra3* (5.8%, $n = 2$ of 34), which is known to mediate itch-evoked responses to chloroquine, was not or rarely detected, while 47.0% ($n = 16$ of 34) of cells expressed *Mrgprd*. *Calca* was detected in the

majority of small-sized TG neurons (61.7%, n = 21 of 34). Especially, I focused on the two subgroups based on co-expression of either ‘*Calca, Trpa1, Trpv1, and Trpc3*’ or ‘*Calca, Mrgpra3, Mrgprd, and Trpc3*’. In *Trpc3*-positive small-sized TG neurons, *Trpa1* and *Trpv1* were found in half (n = 6 of 12) and 33.3% (n = 4 of 12), respectively, suggesting that these receptors were highly co-expressed with *Trpc3* (**Table 3, Figure 20A, and 20C**). Furthermore, *Trpc3* was not only highly co-expressed in *Mrgprd* (n = 9 of 16) but also in *Mrgpra3* (n = 2 of 2) (**Figure 20B, 20C, and Table 3**). Data indicate that *Mrgprd* and *Mrgpra3* are co-expressed with *Trpc3* in small-sized TG neurons.

Overproduced mROS mediate dry skin-induced chronic itch through TRPC3

Next, I investigated whether the mROS level of the affected skin was altered in the dry skin-induced itch model, and also determined the contribution of mROS and TRPC3 in dry skin-induced chronic itch. The experimental procedure is illustrated in **Figure 21**. I established that repeated AEW treatments elicited robust scratching behavior. ID injection of either MitoTEMPO (100 μ mol/L) or Pyr10 (10 μ mol/L or 25 μ mol/L) inhibited the scratching compared to the vehicle group (0.25% DMSO, ** $p < 0.01$, *** $p < 0.001$, and * $p < 0.05$, respectively, unpaired t -test, n = 7-12 per group, **Figure 22**). In addition, improving mitochondrial function and biogenesis by repeated treatment with resveratrol, which is a mitochondrial biogenesis enhancer, (25-30 mg/kg; twice per day) markedly attenuated scratching compared to the vehicle-treated group (5% DMSO, $p < 0.001$, unpaired t -test, n = 7-12 per group, **Figure 22**). The average intensity of MitoSox-Red in the epidermis of AEW-

treated dry skin was remarkably increased compared to naive tissue, but not in the dermis ($p < 0.05$, unpaired t -test, $n = 4-5$ per group, **Figure 23, 24A, and 24B**). Furthermore, the observed thickness of stained epidermis showed an apparent increase in intensity compared to control tissue ($p < 0.001$, unpaired t -test, **Figure 24C**). These results demonstrated the involvement of mROS and TRPC3 in dry skin-induced chronic itch.

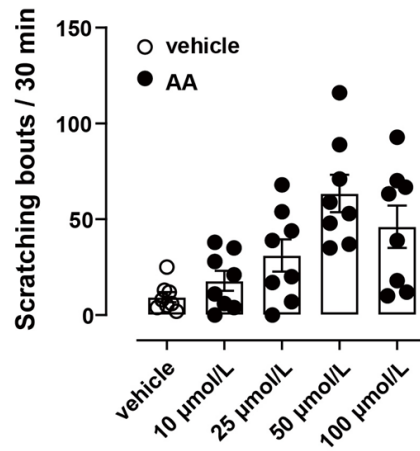


Figure 6. AA induces scratching behavior

i.d. injection of AA (10, 25, 50, and 100 $\mu\text{mol/L}$) elicits scratching behavior for 30 min ($n = 8$ per group). The concentration of peak response is 50 $\mu\text{mol/L}$.

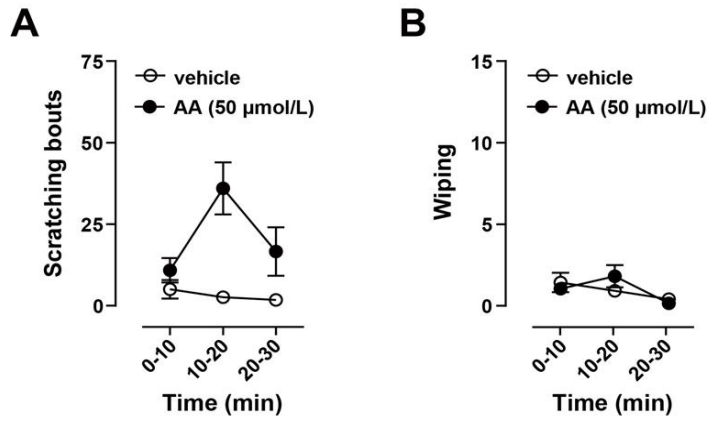


Figure 7. Time courses of scratching (A) and wiping (B)

AA-induced scratching behavior is solely itching without wiping behavior. The response peaks between 10 and 20 min after injection, and then weakens afterward.

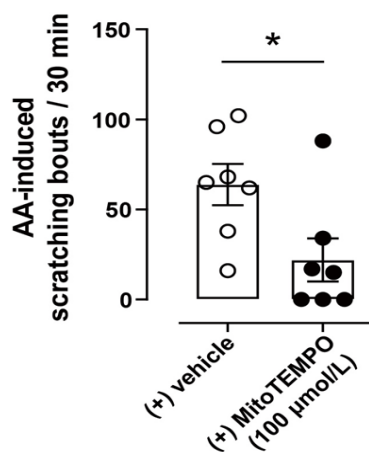


Figure 8. MitoTEMPO reduces AA-induced scratching behavior

AA-induced scratching behavior is markedly suppressed by co-injection with a mitochondria-selective ROS scavenger, MitoTEMPO (100 μ mol/L), but not with PBS-vehicle (n = 7 per group). Data are represented as the mean \pm SEM. * $p < 0.05$.

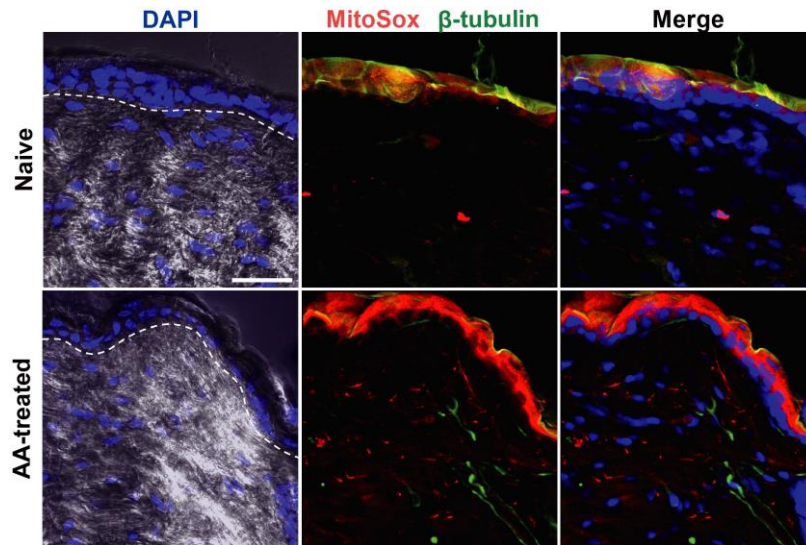


Figure 9. Increased mROS in AA-treated skin

Cell nuclei, nerve fibers and mROS in control and AA-treated cheek skin are stained by DAPI (blue), β -tubulin III (green), and MitoSox-Red (red), respectively (overlays in far-left panels; white dotted lines, epidermal-dermal junction; scale bar, 40 μ m; DIC).

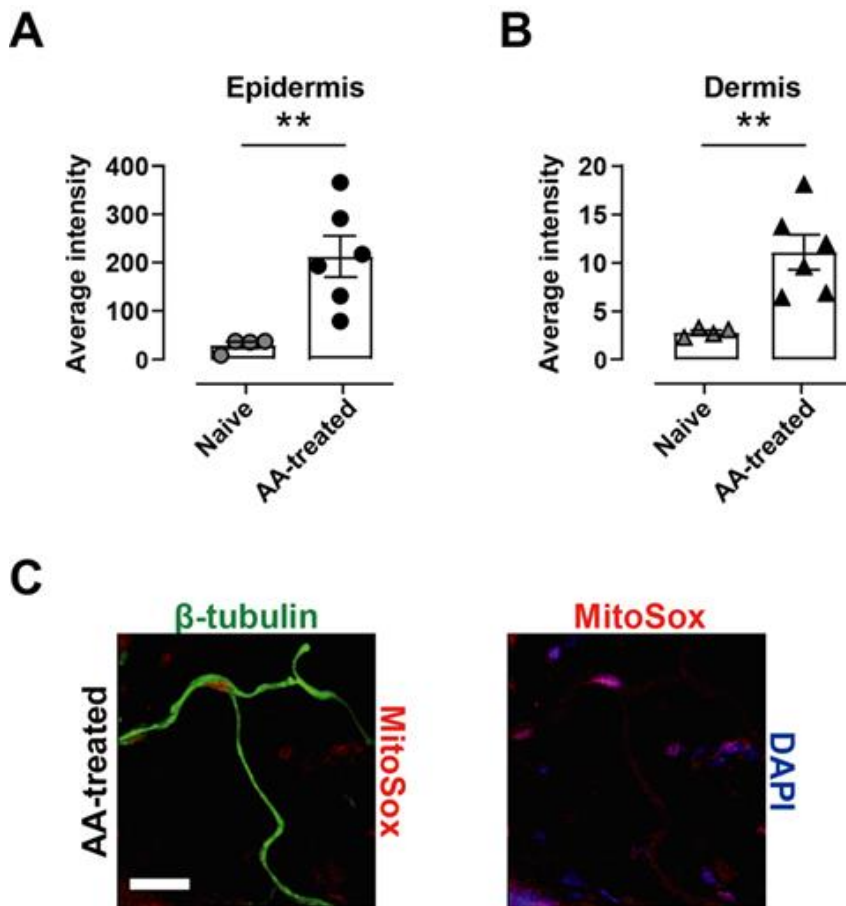


Figure 10. Increased mROS in AA-treated skin and nerve fibers revealed by immunohistochemical analysis

(A, B) The average intensities of MitoSox-Red in epidermis and dermis are markedly elevated by AA treatment. (C) MitoSox-Red co-labeled with β -tubulin III is detected along nerve fibers in the dermis. Data are represented as the mean \pm SEM. ** $p < 0.01$.

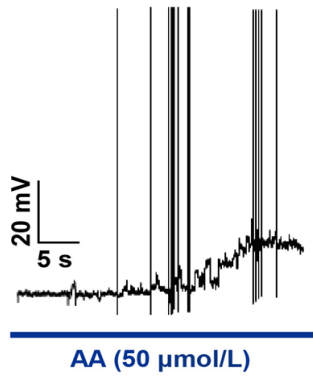


Figure 11. Representative trace of AA-induced action potentials mROS evoked by 50 μ mol/L AA-induced mitochondrial dysfunction activates TG neurons using whole-cell patch clamp recordings.

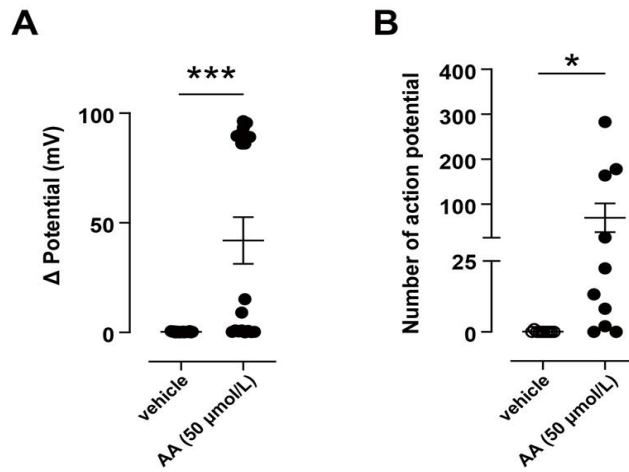


Figure 12. Overproduction of mROS by AA treatment depolarizes the membrane potential in small-sized TG neurons

(A, B) Changes of membrane potential and number of action potentials by 50 $\mu\text{mol/L}$ AA, compared to vehicle (0.05% DMSO, $n = 10-18$ per group). Data are represented as the mean \pm SEM. * $p < 0.05$, *** $p < 0.001$.

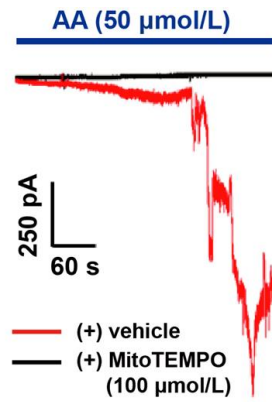


Figure 13. Overproduction of mROS by AA treatment evokes inward currents in small-sized TG neurons

Representative trace of 50 $\mu\text{mol/L}$ AA-induced inward currents in the presence of 100 $\mu\text{mol/L}$ MitoTEMPO or PBS-vehicle.

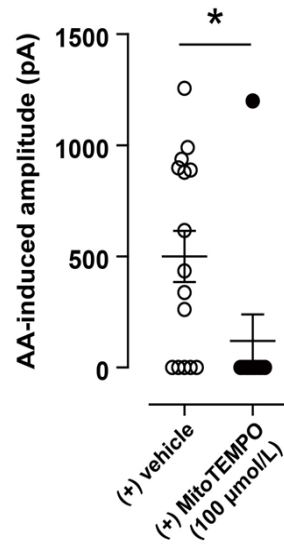


Figure 14. ROS scavenger inhibits AA-induced currents in small-sized TG neurons

AA-induced currents are markedly blocked by MitoTEMPO (100 μ mol/L), compared to vehicle (n = 10–15 per group). Data are represented as the mean \pm SEM. * $p < 0.05$.

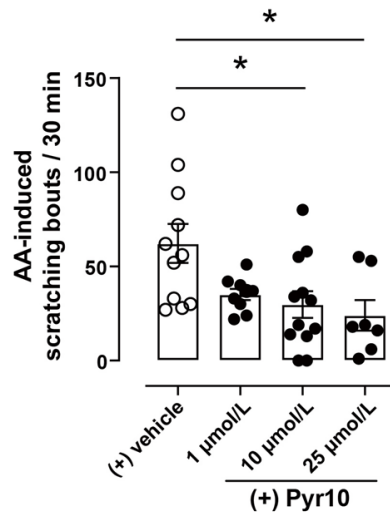


Figure 15. AA-induced scratching is TRPC3-dependent

AA-induced scratching bouts are suppressed by co-injection with Pyr 10 (10 and 25 $\mu\text{mol/L}$), a selective TRPC3 blocker, compared to vehicle (0.25% DMSO, $n = 7-9$ per group). Data are represented as the mean \pm SEM. * $p < 0.05$.

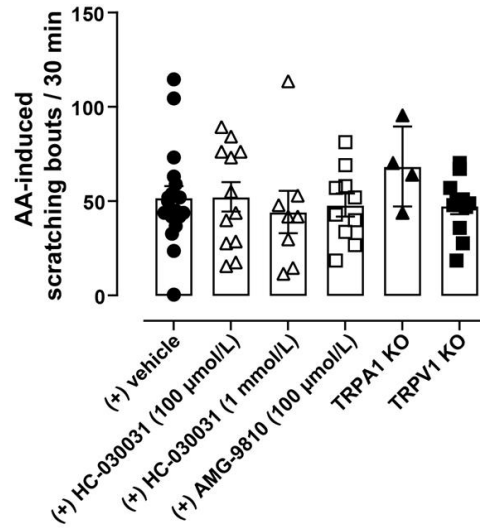


Figure 16. AA-induced scratching is independent of TRPA1 and TRPV1

AA-induced scratching bouts are not affected by co-injection with HC-030031 (100 μ mol/L or 1 mmol/L), a selective TRPA1 blocker, or AMG-9810 (100 μ mol/L), a selective TRPV1 blocker, compared to the vehicle group (0.25% DMSO). TRPA1 KO and TRPV1 KO mice show similar AA-induced scratching behavior, compared to vehicle group (n = 4-18 per group).

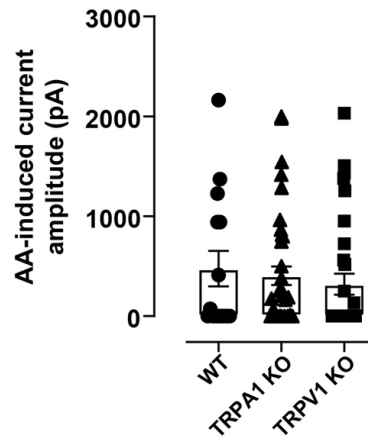


Figure 17. AA-induced inward currents are independent of TRPA1 and TRPV1

AA-induced currents are not different in TRPA1 KO and TRPV1 KO as increased wild-type mice (n = 4-12 per group).

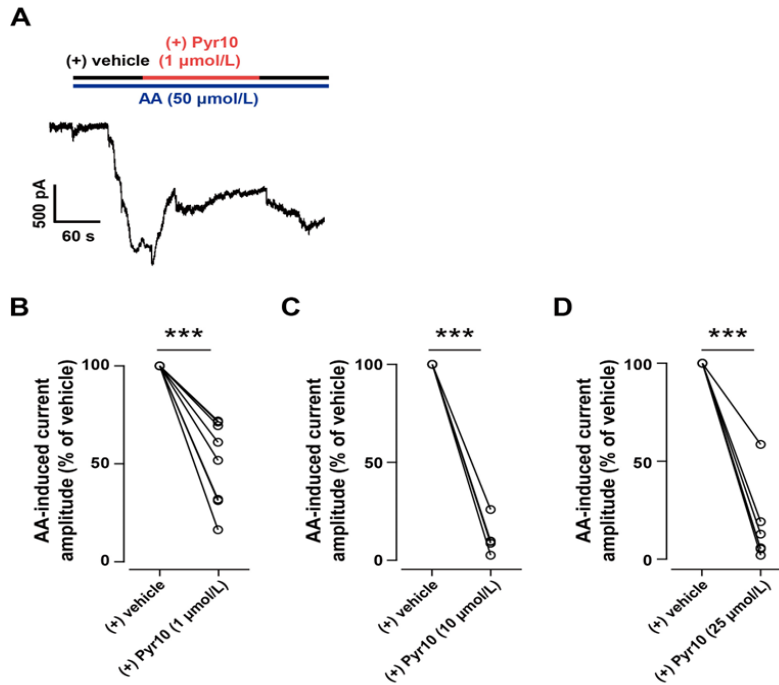


Figure 18. AA-induced currents are TRPC3-dependent

(A) Representative trace of 50 $\mu\text{mol/L}$ AA-induced inward current, which is blocked by 1 $\mu\text{mol/L}$ Pyr10, a selective TRPC3 blocker. AA-induced inward currents are markedly inhibited by (B) 1 $\mu\text{mol/L}$, (C) 10 $\mu\text{mol/L}$, and (D) 25 $\mu\text{mol/L}$ of Pyr10 ($n = 5\text{--}8$ per group). Data are represented as the mean \pm SEM. *** $p < 0.001$.

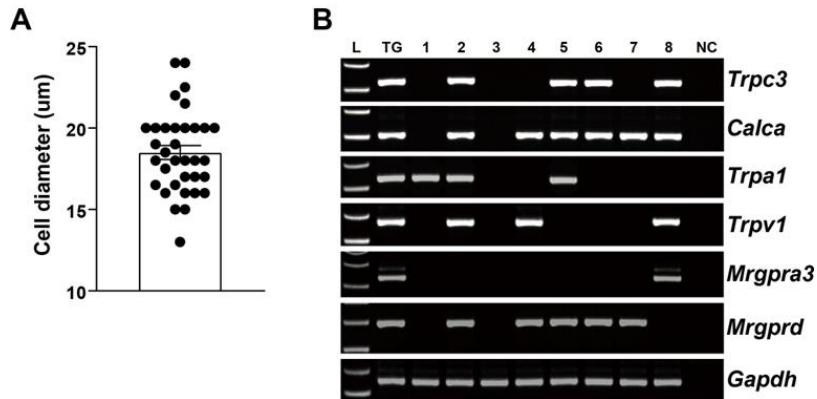


Figure 19. Representative expression pattern of itch-related mediators and receptors mRNAs in individual small-sized TG neurons by scRT-PCR.

(A) An average of cell diameter ($18.50 \pm 0.44 \mu\text{m}$) in small-sized TG neurons collected for scRT-PCR. (B) Gel image showing itch-related mediators and receptors mRNAs. Predicted product sizes are *Trpc3* (210 bp), *Calca* (187 bp), *Trpa1* (219 bp), *Trpv1* (248 bp), *Mrgpra3* (218 bp), and *Mrgprd* (277 bp). Lane L; ladder (DNA size marker), Lane TG; TG tissue, Lanes 1–8; individual TG neurons, Lane NC; negative control.

Gene	No. Cell	1	2	3	4	5	6	7	8	9	10	11	12	13	14	15	16	17	18	19	20	21	22	23	24	25	26	27	28	29	30	31	32	33	34	Expr. %	Expr. % in <i>Trpc3</i> cells	Co-expr. % with <i>Trpc3</i>	
<i>Trpc3</i>		○	○	○	○	○	○	○	○	○	○	○	○				○	○	○	○	○	○	○	○											12/34 (35.2%)	12/12 (100%)	12/12 (100%)		
<i>Calca</i>		○	○	○	○	○	○	○	○	○	○	○	○	○			○	○	○	○	○	○	○	○	○											21/34 (61.7%)	10/12 (83.3%)	10/21 (47.6%)	
<i>Trpa1</i>		○	○	○	○	○	○	○	○	○	○	○	○	○			○	○	○	○	○	○	○	○	○											11/34 (32.3%)	6/12 (50.0%)	6/11 (54.5%)	
<i>Trpv1</i>		○	○	○	○	○	○	○	○	○	○	○	○	○											○											8/34 (23.5%)	4/12 (33.3%)	4/8 (50.0%)	
<i>Mrgpra3</i>		○	○	○	○	○	○	○	○	○	○	○	○	○												○											2/34 (5.8%)	2/12 (16.6%)	2/2 (100%)
<i>Mrgprd</i>		○	○	○	○	○	○	○	○	○	○	○	○	○											○	○	○	○	○	○	○	○	○	○	○		16/34 (47.0%)	9/12 (75.0%)	9/16 (56.2%)
<i>Gapdh</i>		○	○	○	○	○	○	○	○	○	○	○	○	○	○	○	○	○	○	○	○	○	○	○	○	○	○	○	○	○	○	○	○	○	○		34/34 (100%)	12/12 (100%)	12/34 (35.2%)

Table 3. Expression of itch-related mediators and receptors including *Trpc3*, *Calca*, *Trpa1*, *Trpv1*, *Mrgpra3*, and *Mrgprd* in individual small-sized TG neurons by scRT-PCR.

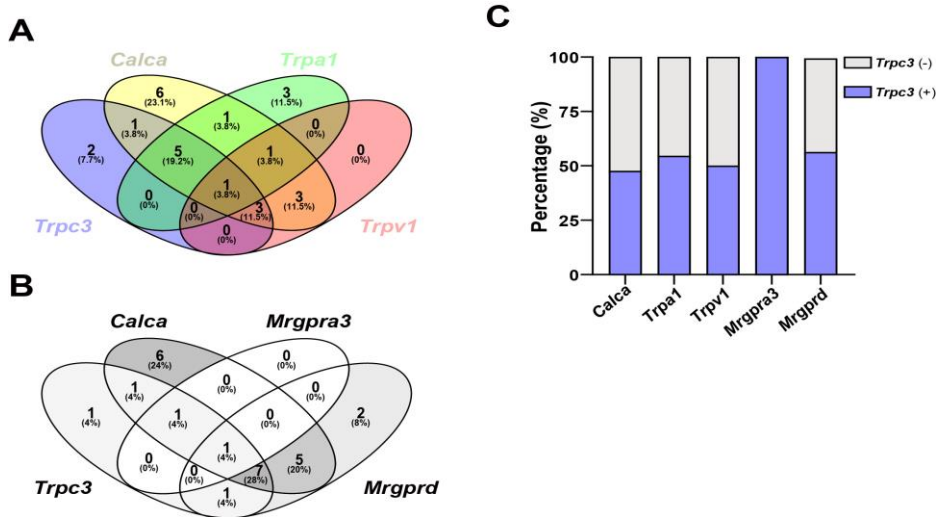


Figure 20. TRPC3 co-expresses itch-related mediators and receptors in small-sized TG neurons.

(A, B) Venn diagrams illustrating the mutual relationship of *Trpc3*⁺, *Calca*⁺, *Trpa1*⁺, *Trpv1*⁺, *Mrgpra3*⁺, and *Mrgprd*⁺. The number of neurons is shown for each population and was obtained from a total of 34 small-sized TG neurons. (C) Patterns of co-expression with *Trpc3* in different itch-related mediators and receptors.

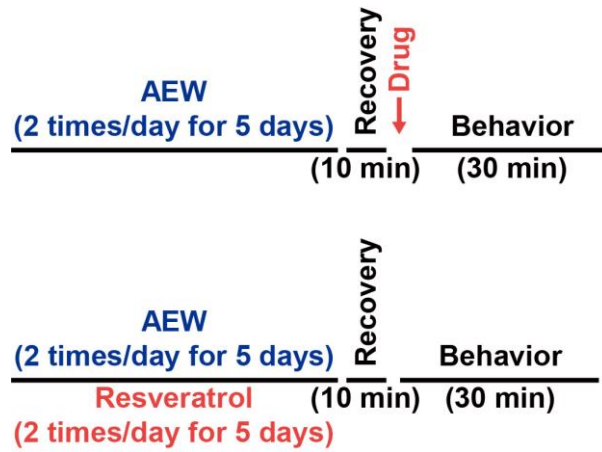


Figure 21. Experimental designs used for dry skin–induced chronic itch model.

AEW was applied to the surface of the skin for chronic dry skin model with itch. Resveratrol was *i.p.* injected.

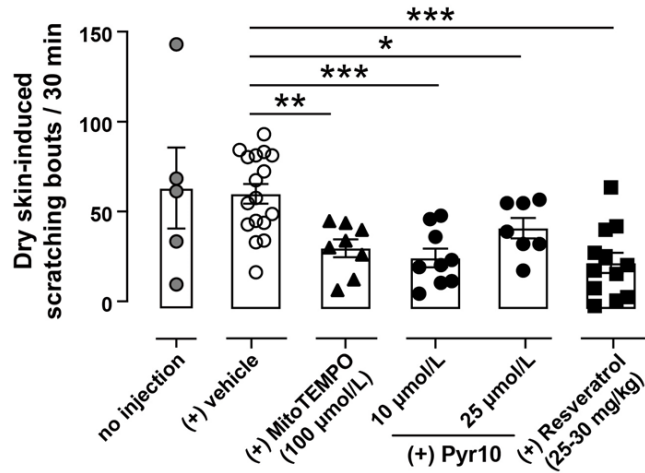


Figure 22. mROS and TRPC3 contribute to dry skin–induced chronic itch.

Dry skin–induced scratching is elicited by repeated AEW treatments, and this is attenuated by *i.d.* injection of MitoTEMPO (100 μ mol/L), a mitochondria–selective ROS scavenger, or Pyr10 (10 and 25 μ mol/L), a selective TRPC3 blocker, compared to the vehicle–treated group (0.25% DMSO, n = 7–12 per group). Repeated *i.p.* injection of resveratrol, a mitochondrial biogenesis enhancer, suppresses dry skin–induced scratching compared to vehicle–treated control (5% DMSO, n = 7–12 per group). Data are represented as the mean \pm SEM. * $p < 0.05$, ** $p < 0.01$, *** $p < 0.001$.

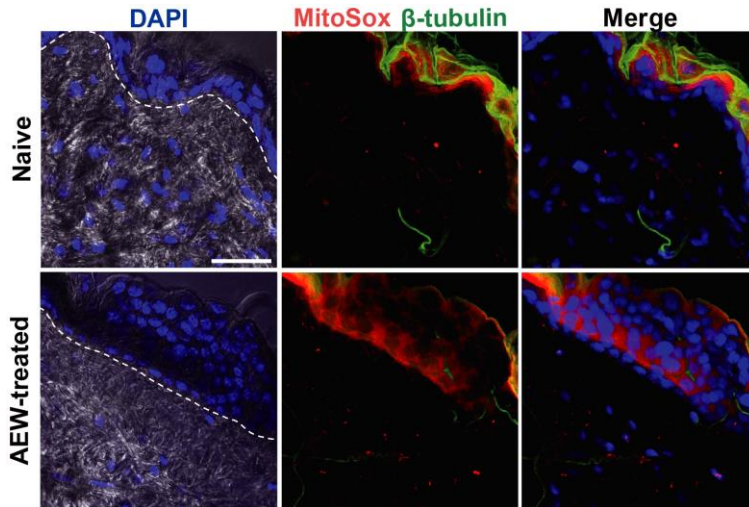


Figure 23. Increase of mROS and thickness in epidermis of AEW-treated skin revealed by immunohistochemical analysis.

Cell nuclei, nerve fibers, and mROS in control and AEW-treated cheek skin stained by DAPI (blue), β -tubulin III (green), and MitoSox-Red (red), a mitochondria-targeted ROS indicator (overlays in far-left panels; white dotted lines, the epidermal-dermal junction; scale bar, 40 μ m; DIC).

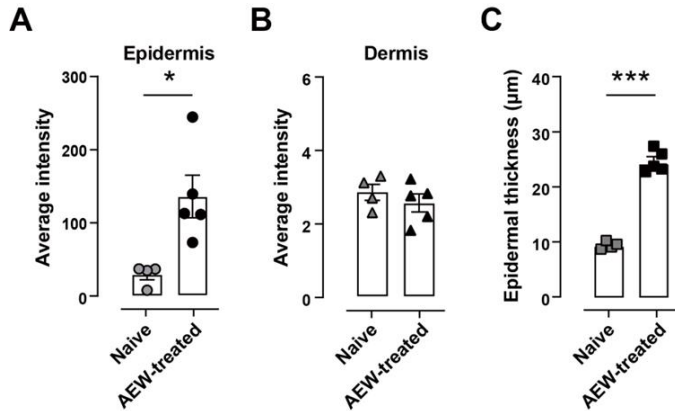


Figure 24. Increased average intensity of MitoSox-Red and thickness in epidermis.

The average intensity of MitoSox-Red in (A) epidermis, but not (B) dermis, is elevated in the dry skin itch model compared to control tissue (n = 4-5 per group). (C) Epidermal thickness of AEW-treated skin is increased compared to control tissue (n = 4-5 per group). Data are represented as the mean \pm SEM. * $p < 0.05$, *** $p < 0.001$.

Discussion

Itch (or pruritus) is defined as an unpleasant sensation which evokes the impulse to scratch, and is one of the most common dermatological complaints of patients. Although the most studied and well-characterized pruritogen is histamine, anti-histamine treatment is of limited efficacy in most types of chronic itch [82], indicating the involvement of complex underlying mechanisms. I demonstrated in this study that mitochondrial modulation by inhibiting mETC complex III using AA induces acute itch behavior through TRPC3, and overproduced mROS from malfunctioning mitochondria elicit dry skin-induced chronic itch via TRPC3. These findings reveal that the TRPC3 channel is a potential target for the treatment of chronic itch.

Overproduction of mROS excites small-sized TG neurons to elicit itch, but not pain

It is known that mitochondria are densely packed at the peripheral terminals of sensory nerves [83] and one of the most common consequences of mitochondrial dysfunction is the overproduction of mROS from the mETC [33, 34]. Although previous studies have indicated that ROS were differentially involved in both pain and itch under pathophysiological conditions [44, 84], it is yet to be determined whether mROS cause pain and/or itch. I found that ID injection of AA, which is known to generate ROS by inhibiting mETC complex III [85], elicited only robust scratching behavior in naive mice, suggesting that AA-induced mROS mediate itch, but not pain (**Figure 7**).

The scratching was suppressed by an mROS-specific scavenger

(Figure 8). These findings indicate that local elevation of mROS generation by mitochondrial modulation in nerve terminals and surrounding skin cells is sufficient to excite primary afferent neurons to elicit itch. In accordance with a previous study showing that ROS and antioxidant proteins are more abundant in the murine epidermis than the dermis [86], I found that the mROS level in the epidermis was about 20-fold higher than that in the dermis in both control and AA-treated tissue **(Figure 10A and 10B)**. In addition, the hyperexcitability of primary afferent neurons elicited by local mROS overproduction is supported by a previous study [37, 38] showing that peripheral application of AA activates bronchopulmonary C-fibers via the selective gating of TRPA1 in a mouse *ex vivo* lung vagal ganglia preparation.

The effect of AA on behavioral outcome has been evaluated in previous studies. Although intrathecal injection of AA results in mechanical hypersensitivity in naive mice [43], *i.d.* injection of AA into the hind paw significantly attenuates the mechanical hypersensitivity caused by some forms of HIV/acquired immune deficiency syndrome therapy, cancer chemotherapy, and diabetes induced neuropathy [87, 88]. AA also alleviates the mechanical hypersensitivity in certain inflammatory pain models [44], implying the involvement of mitochondrial function in pain signaling under pathological conditions. However, itch behavior by peripheral application of AA has not yet been reported. In this study, results showed that *i.d.* injection of AA induced itch exclusively, without wiping behavior **(Figure 6 and 7)**, which is indicative of pain and has been reported following injection of algogenic substances such as capsaicin [73]. Taken together with a previous study, in which *i.d.* injection of oxidants such as H₂O₂ and *tert*-butyl hydroperoxide led

to much more prominent itch than pain [81], it is likely that itch is the major behavioral response to elevated mROS production in peripheral skin tissue at least in the concentration range of drugs tested. Although 20 μ mol/L of AA is almost the maximal dose for mETC complex III inhibition according to previous studies [89, 90], it remained necessary to test whether a higher dose of AA could result in more evident pain in an *in vivo* system. My result revealed that a higher dose (50 μ mol/L) of AA only elicited itching behavior but not pain behavior (**Figure 7**).

TRPC3, but neither TRPA1 nor TRPV1, mediates mROS-induced itch and inward currents

Results showed that local blockade of TRPC3 markedly inhibited AA-induced itch (**Figure 15**) and inward currents (**Figure 18**), suggesting that TRPC3 contributes to itch resulting from mitochondrial dysfunction and subsequent mROS overproduction. TRPC3 belongs to the TRPC family (TRPC1–TRPC7), whose members assemble as homo- or heterotetramers to form non-selective Ca^{2+} -permeable cation channels. Recent studies have reported that TRPC4 is involved in selective serotonin reuptake inhibitor-induced itch [91] and TRPC3 might be a good candidate for mediating β -alanine and cholestatic itch in addition to TRPA1 [92]. In contrast, a previous study has reported that TRPC3 is not required for β -alanine-induced acute pruritus [93]. On the other hand, accumulating evidence indicates that TRPC channels, including TRPC3, are activated by ROS [61–63, 94]. Although a previous study proposed that TRPC3 and TRPC4 contribute subunits to the redox-sensitive channel in endothelial cells [61], it still remains

elusive whether co-expression of TRPC4 is required for ROS sensing by TRPC3 in peripheral sensory systems, considering that the gene expression of TRPC4 is very low in mouse DRG neurons [95] and I found a high incidence of AA-induced current that was completely blocked by a TRPC3-specific blocker in wild-type mice (**Figure 18**).

Pain and itch sensation are known to be conveyed via the same primary afferent neurons, called nociceptive neurons [15], with which the nerves to the TG are densely packed [96]. Nociceptive neurons are categorized into two types: peptidergic neurons expressing neuropeptides such as substance P or CGRP, and non-peptidergic neurons expressing IB4 [97, 98]. scRT-PCR results showed that itch-related mediators and receptors in pruriceptive primary afferent TG neurons were co-expressed with *Trpc3* (**Figure 19 and 20**), suggesting that TRPC3 contributes to itch resulting from mitochondrial dysfunction and subsequent mROS overproduction. TRPC3 is known to be expressed in non-peptidergic small-diameter sensory neurons [95, 99, 100] and is found almost exclusively in MrgprA3⁺ and MrgprD⁺ cells [93]. MrgprA3 receptors directly activated by chloroquine evoke scratching behavior in mice [101] and MrgprD mediates β -alanine-induced itch sensations [64]. In accordance with the previous study, these data showed co-expression of *Trpc3* in *Mrgpra3* (100%, n = 2 of 2) and in *Mrgprd* (56.2%, n = 9 of 16) in small TG neurons (**Figure 19, 20B, and Table 2**).

Also, TRPC3 is co-localized with MrgprA3 and is responsible for the chloroquine-induced excitation of TRPA1-negative DRG neurons, implying the involvement of TRPC3 acting along with TRPA1 to mediate chloroquine-induced itch [65]. Although it is well

known that TRPV1 is involved in histaminergic itch [11], TRPA1 plays a crucial role in acute non-histaminergic itch [10] and MrgprA3 is important for non-histaminergic and TRPV1-independent itch [10], I showed that AA-induced itch was independent of both TRPA1 and TRPV1 (**Figure 16 and 17**) which are also ROS-sensitive and activated by AA [37]. The results seem contradictory to a previous report which showed that ID-injected H₂O₂ elicits robust itch that is blocked by a TRPA1-selective antagonist or in TRPA1 KO mice [81]. This apparent discrepancy might be resolved as follows: (1) In my study, drugs were injected into cheek rather than back skin, implying a possible difference between the trigeminal and spinal itch transduction systems. For example, it has not yet been thoroughly determined whether the expression patterns of various itch-related receptors in TG neurons were similar to DRG neurons. (2) I used AA to generate excessive ROS specifically from intracellular mitochondria, whereas a single type of oxidant was exogenously injected in a previous study. It is not clear whether exogenously-injected oxidant mimics the action of ROS elicited from intracellular mitochondria *in vivo*, considering that ROS are extremely reactive. (3) The actual production levels of mROS by inhibiting mETC III are not clear in the *in vivo* system. In this study, behavior and electrophysiology data (**Figure 15–18**) indicate a functional role of TRPC3 in mROS-evoked itch.

Although I showed the role of TRPC3 in mROS-evoked itch, it remains to be determined how intracellular mROS activates TRPC3 to induce itch. There are at least two possible mechanisms for mROS-induced TRPC3 activation. First, mROS may directly activate TRPC3 through modification of cysteine residues, like its action on other channels such as TRPA1, TRPC5, and TRPV1 [60]. On the

other hand, given that the scRT-PCR revealed that TRPC3 was co-expressed with itch-related MrgprA3 (**Figure 19, 20B, and 20C**), mROS might modulate TRPC3 activation through downstream pathways, like PLC β 3, PKC, and MAPK, which are known to activate TRPA1 [65, 102, 103]. Further work is required to confirm the underlying molecular mechanisms of ROS-mediated TRPC3 activation to produce itch.

mROS and TRPC3 are involved in dry skin-induced chronic itch

It was demonstrated that ID injection of an mROS specific scavenger markedly inhibited dry skin-induced itch (**Figure 22**), suggesting that mROS plays a crucial role in chronic itch. Several lines of evidence further support the idea that malfunction of mitochondria is one important factor in various kinds of chronic itch. First, mitochondrial dysfunction is involved in skin diseases accompanied by chronic itch such as psoriasis and atopic dermatitis [104, 105]. Second, some other diseases associated with mitochondrial dysfunction, but not directly related to skin disorders, e.g., diabetes, chronic liver diseases, cholestasis, and peripheral neuropathy, also frequently accompany chronic itch [40, 106–108]. Third, itch is a predominant skin complaint especially in the elderly who are usually more prone to dry skin than younger people. It is widely accepted that aging is associated with mitochondrial dysfunction and increased ROS production [109]. Here, the data showing that repeated treatment with resveratrol, a mitochondrial biogenesis enhancer, markedly suppressed dry skin-induced itch (**Figure 22**) are also in good accordance with the critical role of mitochondrial function in chronic itch.

Dry skin-induced chronic scratching was also significantly relieved by blocking of TRPC3 in skin tissue (**Figure 22**), indicating that TRPC3 mediates, at least in part, dry skin-induced chronic itch. This was not surprising, considering that mROS-induced itch (**Figure 15**) and mROS-induced inward current (**Figure 18**) were suppressed by a TRPC3-selective blocker. Furthermore, specific innervation of nerve fibers with MrgprA3 [101] and MrgprD [110] in the epidermis, and enhanced non-peptidergic intra-epidermal fiber density in a dry skin-induced itch model [111] support the hypothesis that TRPC3 contributes to dry skin-induced chronic itch. However, co-expression or interaction with TRPA1, which has been suggested to be a key player in dry skin itch [56], and other itch receptors remain to be determined. The activation of TRPC3 by diverse pruritogens, e.g., histamine [112], 5-HT [113], and chloroquine [65], further raises the possibility that TRPC3 is also an important player in various other itchy conditions.

It is interesting to note the differential expression of mROS between AA-treated and AEW-treated mice. The MitoSox signal was highly expressed in the epidermal layer in both AA-treated (**Figure 9 and 10A**) and AEW-treated mice (**Figure 23 and 24A**). However, the MitoSox signal significantly increased along nerve fibers in the dermal layer in AA-treated mice (**Figure 9, 10B, and 10C**) while AEW treatment had no effect on mROS expression in the dermis (**Figure 23 and 24B**). The discrepancy in the expression of mROS between the two models might be due to the different routes of drug application. ID injection of AA directly exposed the dermis to the drug and might lead to the production of mROS. On the contrary, the dermis of AEW-treated mice was unaffected as the drug (i.e., AEW) was applied to the surface of the skin.

Conclusion

To conclude, my results indicated that locally elevated mROS production by mitochondrial dysfunction elicited itch through TRPC3, which might be one of underlying mechanisms of chronic itch. Given that mitochondrial dysfunction and mROS overproduction are broadly associated with diseases accompanying chronic itch and that TRPC3 is activated by diverse pruritogens [65, 112, 113], pharmacological approaches that restore mitochondrial function and block excessive mROS or TRPC3 might be considered to relieve various types of chronic itch.

References

- [1] Ringkamp M, Schepers RJ, Shimada SG, Johanek LM, Hartke TV, Borzan J, et al. A role for nociceptive, myelinated nerve fibers in itch sensation. *J Neurosci* 2011, 31: 14841–14849.
- [2] Graham HT, Lowry OH, Wahl N, Priebat MK. Mast cells as sources of tissue histamine. *J Exp Med* 1955, 102: 307–318.
- [3] Shimizu K, Andoh T, Yoshihisa Y, Shimizu T. Histamine released from epidermal keratinocytes plays a role in alpha-melanocyte-stimulating hormone-induced itching in mice. *Am J Pathol* 2015, 185: 3003–3010.
- [4] Wang F, Trier AM, Li F, Kim S, Chen Z, Chai JN, et al. A basophil-neuronal axis promotes itch. *Cell* 2021, 184: 422–440 e417.
- [5] Yosipovitch G, Greaves MW, Schmelz M. Itch. *Lancet* 2003, 361: 690–694.
- [6] Sharma L. Diagnostic clinical features of atopic dermatitis. *Indian J Dermatol Venereol Leprol* 2001, 67: 25–27.
- [7] Choi S, Lee K, Jung H, Park N, Kang J, Nam KH, et al. Kruppel-Like Factor 4 Positively Regulates Autoimmune Arthritis in Mouse Models and Rheumatoid Arthritis in Patients via Modulating Cell Survival and Inflammation Factors of Fibroblast-Like Synoviocyte. *Front Immunol* 2018, 9: 1339 1–12.
- [8] Krajnik M, Zylicz Z. Understanding pruritus in systemic disease. *J Pain Symptom Manage* 2001, 21: 151–168.
- [9] Han SK, Mancino V, Simon MI. Phospholipase Cbeta 3 mediates the scratching response activated by the histamine H1 receptor on C-fiber nociceptive neurons. *Neuron* 2006, 52: 691–703.

- [10] Wilson SR, Gerhold KA, Bifulco-Fisher A, Liu Q, Patel KN, Dong X, et al. TRPA1 is required for histamine-independent, Mas-related G protein-coupled receptor-mediated itch. *Nat Neurosci* 2011, 14: 595–602.
- [11] Kim BM, Lee SH, Shim WS, Oh U. Histamine-induced Ca^{2+} influx via the PLA(2)/lipoxygenase/TRPV1 pathway in rat sensory neurons. *Neurosci Lett* 2004, 361: 159–162.
- [12] Bautista DM, Jordt SE, Nikai T, Tsuruda PR, Read AJ, Poblete J, et al. TRPA1 mediates the inflammatory actions of environmental irritants and proalgesic agents. *Cell* 2006, 124: 1269–1282.
- [13] Caterina MJ, Leffler A, Malmberg AB, Martin WJ, Trafton J, Petersen-Zeitz KR, et al. Impaired nociception and pain sensation in mice lacking the capsaicin receptor. *Science* 2000, 288: 306–313.
- [14] Caterina MJ, Schumacher MA, Tominaga M, Rosen TA, Levine JD, Julius D. The capsaicin receptor: a heat-activated ion channel in the pain pathway. *Nature* 1997, 389: 816–824.
- [15] Ikoma A, Steinhoff M, Stander S, Yosipovitch G, Schmelz M. The neurobiology of itch. *Nat Rev Neurosci* 2006, 7: 535–547.
- [16] Mishra SK, Hoon MA. The cells and circuitry for itch responses in mice. *Science* 2013, 340: 968–971.
- [17] Sun YG, Chen ZF. A gastrin-releasing peptide receptor mediates the itch sensation in the spinal cord. *Nature* 2007, 448: 700–703.
- [18] Chen XJ, Sun YG. Central circuit mechanisms of itch. *Nat Commun* 2020, 11: 3052 1–10.
- [19] Ross SE, Mardinly AR, McCord AE, Zurawski J, Cohen S, Jung C, et al. Loss of inhibitory interneurons in the dorsal spinal cord and elevated itch in *Bhlhb5* mutant mice. *Neuron* 2010, 65: 886–898.

- [20] Yosipovitch G, Ishiujji Y, Patel TS, Hicks MI, Oshiro Y, Kraft RA, et al. The brain processing of scratching. *J Invest Dermatol* 2008, 128: 1806–1811.
- [21] Mochizuki H, Tashiro M, Kano M, Sakurada Y, Itoh M, Yanai K. Imaging of central itch modulation in the human brain using positron emission tomography. *Pain* 2003, 105: 339–346.
- [22] Mochizuki H, Kakigi R. Central mechanisms of itch. *Clin Neurophysiol* 2015, 126: 1650–1660.
- [23] Adam–Vizi V. Production of reactive oxygen species in brain mitochondria: contribution by electron transport chain and non–electron transport chain sources. *Antioxid Redox Signal* 2005, 7: 1140–1149.
- [24] Miyata Y, Mukae Y, Harada J, Matsuda T, Mitsunari K, Matsuo T, et al. Pathological and Pharmacological Roles of Mitochondrial Reactive Oxygen Species in Malignant Neoplasms: Therapies Involving Chemical Compounds, Natural Products, and Photosensitizers. *Molecules* 2020, 25: 5252 1–21.
- [25] Aon MA, Cortassa S, O'Rourke B. Redox–optimized ROS balance: a unifying hypothesis. *Biochim Biophys Acta* 2010, 1797: 865–877.
- [26] Hu Q, Qin Y, Xiang J, Liu W, Xu W, Sun Q, et al. dCK negatively regulates the NRF2/ARE axis and ROS production in pancreatic cancer. *Cell Prolif* 2018, 51: e12456 1–12.
- [27] Pashkovskaia N, Gey U, Rodel G. Mitochondrial ROS direct the differentiation of murine pluripotent P19 cells. *Stem Cell Res* 2018, 30: 180–191.
- [28] Cheignon C, Tomas M, Bonnefont–Rousselot D, Faller P, Hureau C, Collin F. Oxidative stress and the amyloid beta peptide in Alzheimer's disease. *Redox Biol* 2018, 14: 450–464.

- [29] Robson R, Kundur AR, Singh I. Oxidative stress biomarkers in type 2 diabetes mellitus for assessment of cardiovascular disease risk. *Diabetes Metab Syndr* 2018, 12: 455–462.
- [30] Li J, O W, Li W, Jiang ZG, Ghanbari HA. Oxidative stress and neurodegenerative disorders. *Int J Mol Sci* 2013, 14: 24438–24475.
- [31] Brand MD. Mitochondrial generation of superoxide and hydrogen peroxide as the source of mitochondrial redox signaling. *Free Radic Biol Med* 2016, 100: 14–31.
- [32] Gopcevic KR, Rovcanin BR, Tatic SB, Krivokapic ZV, Gajic MM, Dragutinovic VV. Activity of superoxide dismutase, catalase, glutathione peroxidase, and glutathione reductase in different stages of colorectal carcinoma. *Dig Dis Sci* 2013, 58: 2646–2652.
- [33] Bonawitz ND, Rodeheffer MS, Shadel GS. Defective mitochondrial gene expression results in reactive oxygen species-mediated inhibition of respiration and reduction of yeast life span. *Mol Cell Biol* 2006, 26: 4818–4829.
- [34] Lin MT, Beal MF. Mitochondrial dysfunction and oxidative stress in neurodegenerative diseases. *Nature* 2006, 443: 787–795.
- [35] Nunnari J, Suomalainen A. Mitochondria: in sickness and in health. *Cell* 2012, 148: 1145–1159.
- [36] Holmstrom KM, Finkel T. Cellular mechanisms and physiological consequences of redox-dependent signalling. *Nat Rev Mol Cell Biol* 2014, 15: 411–421.
- [37] Nesuashvili L, Hadley SH, Bahia PK, Taylor–Clark TE. Sensory nerve terminal mitochondrial dysfunction activates airway sensory nerves via transient receptor potential (TRP) channels. *Mol Pharmacol* 2013, 83: 1007–1019.

- [38] Hadley SH, Bahia PK, Taylor–Clark TE. Sensory nerve terminal mitochondrial dysfunction induces hyperexcitability in airway nociceptors via protein kinase C. *Mol Pharmacol* 2014, 85: 839–848.
- [39] Kim HY, Lee KY, Lu Y, Wang J, Cui L, Kim SJ, et al. Mitochondrial Ca^{2+} uptake is essential for synaptic plasticity in pain. *J Neurosci* 2011, 31: 12982–12991.
- [40] Sui BD, Xu TQ, Liu JW, Wei W, Zheng CX, Guo BL, et al. Understanding the role of mitochondria in the pathogenesis of chronic pain. *Postgrad Med J* 2013, 89: 709–714.
- [41] Paliwal S, Chaudhuri R, Agrawal A, Mohanty S. Regenerative abilities of mesenchymal stem cells through mitochondrial transfer. *J Biomed Sci* 2018, 25: 31 1–12.
- [42] Park WH, You BR. Antimycin A induces death of the human pulmonary fibroblast cells via ROS increase and GSH depletion. *Int J Oncol* 2016, 48: 813–820.
- [43] Kim HY, Chung JM, Chung K. Increased production of mitochondrial superoxide in the spinal cord induces pain behaviors in mice: the effect of mitochondrial electron transport complex inhibitors. *Neurosci Lett* 2008, 447: 87–91.
- [44] Joseph EK, Levine JD. Mitochondrial electron transport in models of neuropathic and inflammatory pain. *Pain* 2006, 121: 105–114.
- [45] LaMotte RH, Dong X, Ringkamp M. Sensory neurons and circuits mediating itch. *Nat Rev Neurosci* 2014, 15: 19–31.
- [46] Ward L, Wright E, McMahon SB. A comparison of the effects of noxious and innocuous counterstimuli on experimentally induced itch and pain. *Pain* 1996, 64: 129–138.
- [47] Sun YG, Zhao ZQ, Meng XL, Yin J, Liu XY, Chen ZF. Cellular basis of itch sensation. *Science* 2009, 325: 1531–1534.

- [48] Dong X, Dong X. Peripheral and Central Mechanisms of Itch. *Neuron* 2018, 98: 482–494.
- [49] Han L, Dong X. Itch mechanisms and circuits. *Annu Rev Biophys* 2014, 43: 331–355.
- [50] Liu Y, Abdel Samad O, Zhang L, Duan B, Tong Q, Lopes C, et al. VGLUT2–dependent glutamate release from nociceptors is required to sense pain and suppress itch. *Neuron* 2010, 68: 543–556.
- [51] Lagerstrom MC, Rogoz K, Abrahamsen B, Persson E, Reinius B, Nordenankar K, et al. VGLUT2–dependent sensory neurons in the TRPV1 population regulate pain and itch. *Neuron* 2010, 68: 529–542.
- [52] Bautista DM, Movahed P, Hinman A, Axelsson HE, Sterner O, Hogestatt ED, et al. Pungent products from garlic activate the sensory ion channel TRPA1. *Proc Natl Acad Sci* 2005, 102: 12248–12252.
- [53] Bulley S, Fernandez–Pena C, Hasan R, Leo MD, Muralidharan P, Mackay CE, et al. Arterial smooth muscle cell PKD2 (TRPP1) channels regulate systemic blood pressure. *Elife* 2018, 7: 1–23.
- [54] Minke B, Wu C, Pak WL. Induction of photoreceptor voltage noise in the dark in *Drosophila* mutant. *Nature* 1975, 258: 84–87.
- [55] Walker KM, Urban L, Medhurst SJ, Patel S, Panesar M, Fox AJ, et al. The VR1 antagonist capsazepine reverses mechanical hyperalgesia in models of inflammatory and neuropathic pain. *J Pharmacol Exp Ther* 2003, 304: 56–62.
- [56] Wilson SR, Nelson AM, Batia L, Morita T, Estandian D, Owens DM, et al. The ion channel TRPA1 is required for chronic itch. *J Neurosci* 2013, 33: 9283–9294.
- [57] Imamachi N, Park GH, Lee H, Anderson DJ, Simon MI, Basbaum AI, et al. TRPV1–expressing primary afferents generate behavioral

responses to pruritogens via multiple mechanisms. *Proc Natl Acad Sci U S A* 2009, 106: 11330–11335.

[58] Shirolkar P, Mishra SK. Role of TRP ion channels in pruritus. *Neurosci Lett* 2022, 768: 136379 1–7.

[59] Xiao B, Patapoutian A. Scratching the surface: a role of pain-sensing TRPA1 in itch. *Nat Neurosci* 2011, 14: 540–542.

[60] Ogawa N, Kurokawa T, Mori Y. Sensing of redox status by TRP channels. *Cell Calcium* 2016, 60: 115–122.

[61] Poteser M, Graziani A, Rosker C, Eder P, Derler I, Kahr H, et al. TRPC3 and TRPC4 associate to form a redox-sensitive cation channel. Evidence for expression of native TRPC3–TRPC4 heteromeric channels in endothelial cells. *J Biol Chem* 2006, 281: 13588–13595.

[62] Cioffi DL. Redox regulation of endothelial canonical transient receptor potential channels. *Antioxid Redox Signal* 2011, 15: 1567–1582.

[63] Balzer M, Lintschinger B, Groschner K. Evidence for a role of Trp proteins in the oxidative stress-induced membrane conductances of porcine aortic endothelial cells. *Cardiovasc Res* 1999, 42: 543–549.

[64] Liu Q, Sikand P, Ma C, Tang Z, Han L, Li Z, et al. Mechanisms of itch evoked by beta-alanine. *J Neurosci* 2012, 32: 14532–14537.

[65] Than JY, Li L, Hasan R, Zhang X. Excitation and modulation of TRPA1, TRPV1, and TRPM8 channel-expressing sensory neurons by the pruritogen chloroquine. *J Biol Chem* 2013, 288: 12818–12827.

[66] Yalcin B, Tamer E, Toy GG, Oztas P, Hayran M, Alli N. The prevalence of skin diseases in the elderly: analysis of 4099 geriatric patients. *Int J Dermatol* 2006, 45: 672–676.

- [67] Barzegari A, Nouri M, Gueguen V, Saeedi N, Pavon–Djavid G, Omidi Y. Mitochondria–targeted antioxidant mito–TEMPO alleviate oxidative stress induced by antimycin A in human mesenchymal stem cells. *J Cell Physiol* 2020, 235: 5628–5636.
- [68] Pelizzoni I, Macco R, Morini MF, Zacchetti D, Grohovaz F, Codazzi F. Iron handling in hippocampal neurons: activity–dependent iron entry and mitochondria–mediated neurotoxicity. *Aging Cell* 2011, 10: 172–183.
- [69] Schleifer H, Doleschal B, Lichtenegger M, Oppenrieder R, Derler I, Frischauf I, et al. Novel pyrazole compounds for pharmacological discrimination between receptor–operated and store–operated Ca^{2+} entry pathways. *Br J Pharmacol* 2012, 167: 1712–1722.
- [70] McNamara CR, Mandel–Brehm J, Bautista DM, Siemens J, Deranian KL, Zhao M, et al. TRPA1 mediates formalin–induced pain. *Proc Natl Acad Sci U S A* 2007, 104: 13525–13530.
- [71] Gavva NR, Tamir R, Qu Y, Klionsky L, Zhang TJ, Immke D, et al. AMG 9810 [(E)–3–(4–t–butylphenyl)–N–(2,3–dihydrobenzo[b] [1,4] dioxin–6–yl) acrylamide], a novel vanilloid receptor 1 (TRPV1) antagonist with antihyperalgesic properties. *J Pharmacol Exp Ther* 2005, 313: 474–484.
- [72] Price NL, Gomes AP, Ling AJ, Duarte FV, Martin–Montalvo A, North BJ, et al. SIRT1 is required for AMPK activation and the beneficial effects of resveratrol on mitochondrial function. *Cell Metab* 2012, 15: 675–690.
- [73] Shimada SG, LaMotte RH. Behavioral differentiation between itch and pain in mouse. *Pain* 2008, 139: 681–687.
- [74] Ehling S, Butler A, Thi S, Ghashghaei HT, Baumer W. To scratch an itch: Establishing a mouse model to determine active brain areas involved in acute histaminergic itch. *IBRO Rep* 2018, 5: 67–73.

- [75] Park CK, Kim MS, Fang Z, Li HY, Jung SJ, Choi SY, et al. Functional expression of thermo-transient receptor potential channels in dental primary afferent neurons: implication for tooth pain. *J Biol Chem* 2006, 281: 17304–17311.
- [76] Turrens JF, Alexandre A, Lehninger AL. Ubisemiquinone is the electron donor for superoxide formation by complex III of heart mitochondria. *Arch Biochem Biophys* 1985, 237: 408–414.
- [77] Vesce S, Kirk L, Nicholls DG. Relationships between superoxide levels and delayed calcium deregulation in cultured cerebellar granule cells exposed continuously to glutamate. *J Neurochem* 2004, 90: 683–693.
- [78] Green AD, Young KK, Lehto SG, Smith SB, Mogil JS. Influence of genotype, dose and sex on pruritogen-induced scratching behavior in the mouse. *Pain* 2006, 124: 50–58.
- [79] Liu Q, Tang Z, Surdenikova L, Kim S, Patel KN, Kim A, et al. Sensory neuron-specific GPCR Mrgprs are itch receptors mediating chloroquine-induced pruritus. *Cell* 2009, 139: 1353–1365.
- [80] Liu T, Xu ZZ, Park CK, Berta T, Ji RR. Toll-like receptor 7 mediates pruritus. *Nat Neurosci* 2010, 13: 1460–1462.
- [81] Liu T, Ji RR. Oxidative stress induces itch via activation of transient receptor potential subtype ankyrin 1 in mice. *Neurosci Bull* 2012, 28: 145–154.
- [82] Grundmann S, Stander S. Chronic pruritus: clinics and treatment. *Ann Dermatol* 2011, 23: 1–11.
- [83] Hung KS, Hertweck MS, Hardy JD, Loosli CG. Ultrastructure of nerves and associated cells in bronchiolar epithelium of the mouse lung. *J Ultrastruct Res* 1973, 43: 426–437.

- [84] Sivaranjani N, Rao SV, Rajeev G. Role of reactive oxygen species and antioxidants in atopic dermatitis. *J Clin Diagn Res* 2013, 7: 2683–2685.
- [85] Alexandre A, Lehninger AL. Bypasses of the antimycin A block of mitochondrial electron transport in relation to ubiquinone function. *Biochim Biophys Acta* 1984, 767: 120–129.
- [86] Carr WJ, Oberley–Deegan RE, Zhang Y, Oberley CC, Oberley LW, Dunnwald M. Antioxidant proteins and reactive oxygen species are decreased in a murine epidermal side population with stem cell–like characteristics. *Histochem Cell Biol* 2011, 135: 293–304.
- [87] Joseph EK, Levine JD. Multiple PKCepsilon–dependent mechanisms mediating mechanical hyperalgesia. *Pain* 2010, 150: 17–21.
- [88] Joseph EK, Levine JD. Comparison of oxaliplatin– and cisplatin–induced painful peripheral neuropathy in the rat. *J Pain* 2009, 10: 534–541.
- [89] Gonzalez–Dosal R, Horan KA, Paludan SR. Mitochondria–derived reactive oxygen species negatively regulates immune innate signaling pathways triggered by a DNA virus, but not by an RNA virus. *Biochem Biophys Res Commun* 2012, 418: 806–810.
- [90] Liu M, Liu H, Dudley SC, Jr. Reactive oxygen species originating from mitochondria regulate the cardiac sodium channel. *Circ Res* 2010, 107: 967–974.
- [91] Lee SH, Cho PS, Tonello R, Lee HK, Jang JH, Park GY, et al. Peripheral serotonin receptor 2B and transient receptor potential channel 4 mediate pruritus to serotonergic antidepressants in mice. *J Allergy Clin Immunol* 2018, 142: 1349–1352.
- [92] Sun S, Dong X. Trp channels and itch. *Semin Immunopathol* 2016, 38: 293–307.

- [93] Dong P, Guo C, Huang S, Ma M, Liu Q, Luo W. TRPC3 Is Dispensable for beta-Alanine Triggered Acute Itch. *Sci Rep* 2017, 7: 13869 1–12.
- [94] Takahashi N, Mori Y. TRP Channels as Sensors and Signal Integrators of Redox Status Changes. *Front Pharmacol* 2011, 2: 58.
- [95] Usoskin D, Furlan A, Islam S, Abdo H, Lonnerberg P, Lou D, et al. Unbiased classification of sensory neuron types by large-scale single-cell RNA sequencing. *Nat Neurosci* 2015, 18: 145–153.
- [96] Dixon AD. The ultrastructure of nerve fibers in the trigeminal ganglion of the rat. *J Ultrastruct Res* 1963, 8: 107–121.
- [97] Molliver DC, Radeke MJ, Feinstein SC, Snider WD. Presence or absence of TrkA protein distinguishes subsets of small sensory neurons with unique cytochemical characteristics and dorsal horn projections. *J Comp Neurol* 1995, 361: 404–416.
- [98] Snider WD, McMahon SB. Tackling pain at the source: new ideas about nociceptors. *Neuron* 1998, 20: 629–632.
- [99] Luo W, Wickramasinghe SR, Savitt JM, Griffin JW, Dawson TM, Ginty DD. A hierarchical NGF signaling cascade controls Ret-dependent and Ret-independent events during development of nonpeptidergic DRG neurons. *Neuron* 2007, 54: 739–754.
- [100] Alkhani H, Ase AR, Grant R, O'Donnell D, Groschner K, Seguela P. Contribution of TRPC3 to store-operated calcium entry and inflammatory transductions in primary nociceptors. *Mol Pain* 2014, 10: 43 1–12.
- [101] Han L, Ma C, Liu Q, Weng HJ, Cui Y, Tang Z, et al. A subpopulation of nociceptors specifically linked to itch. *Nat Neurosci* 2013, 16: 174–182.
- [102] Kittaka H, Tominaga M. The molecular and cellular mechanisms of itch and the involvement of TRP channels in the

peripheral sensory nervous system and skin. *Allergol Int* 2017, 66: 22–30.

[103] Giorgi S, Nikolaeva–Koleva M, Alarcon–Alarcon D, Butron L, Gonzalez–Rodriguez S. Is TRPA1 Burning Down TRPV1 as Druggable Target for the Treatment of Chronic Pain? *Int J Mol Sci* 2019, 20 1–20.

[104] Bickers DR, Athar M. Oxidative stress in the pathogenesis of skin disease. *J Invest Dermatol* 2006, 126: 2565–2575.

[105] Feichtinger RG, Sperl W, Bauer JW, Kofler B. Mitochondrial dysfunction: a neglected component of skin diseases. *Exp Dermatol* 2014, 23: 607–614.

[106] Mela M, Mancuso A, Burroughs AK. Review article: pruritus in cholestatic and other liver diseases. *Aliment Pharmacol Ther* 2003, 17: 857–870.

[107] Weisshaar E, Dalgard F. Epidemiology of itch: adding to the burden of skin morbidity. *Acta Derm Venereol* 2009, 89: 339–350.

[108] Oaklander AL. Neuropathic Itch. *Itch: Mechanisms and Treatment* 2014.

[109] Bratic A, Larsson NG. The role of mitochondria in aging. *J Clin Invest* 2013, 123: 951–957.

[110] Zylka MJ, Rice FL, Anderson DJ. Topographically distinct epidermal nociceptive circuits revealed by axonal tracers targeted to Mrgprd. *Neuron* 2005, 45: 17–25.

[111] Valtcheva MV, Samineni VK, Golden JP, Gereau RWt, Davidson S. Enhanced nonpeptidergic intraepidermal fiber density and an expanded subset of chloroquine–responsive trigeminal neurons in a mouse model of dry skin itch. *J Pain* 2015, 16: 346–356.

[112] Kwan HY, Wong CO, Chen ZY, Dominic Chan TW, Huang Y, Yao X. Stimulation of histamine H2 receptors activates TRPC3

channels through both phospholipase C and phospholipase D. *Eur J Pharmacol* 2009, 602: 181–187.

[113] Zhou FM, Lee CR. Intrinsic and integrative properties of substantia nigra pars reticulata neurons. *Neuroscience* 2011, 198: 69–94.

국문초록

미토콘드리아 활성산소종에 의해 유발되는 가려움증에서 감각 신경세포의 transient receptor potential canonical 3의 역할

김 성 아

서울대학교 대학원

치의과학과 신경생물학 전공

(지도교수: 오 석 배)

노화로 인해 피부는 건조해지며 활성산소도 증가한다. 이때 동반되는 피부질환이 가려움증이며, 이러한 가려움증이 만성화될수록 삶의 질이 떨어진다. 히스타민 이외에도 가려움 유발 매개체가 많이 보고되고 있으며 그 기전이 매우 복잡하고 아직 불분명하기 때문에 만성 가려움증 치료에 어려움이 많다. 지금까지 밝혀진 가려움증 기전은 통증 기전과 매우 관련되어 있다. 비록 미토콘드리아의 기능 장애로 인해 증가된 활성산소종인 mROS가 통증을 유발시킨다는 연구는 보고된 바 있으나, 이 mROS가 가려움증에 미치는 영향에 대해서는 알려진 바가 거의 없다. 뿐만 아니라, 통증과 가려움증을 매개하는 대표적인 이온채널인 TRPV1과 TRPA1에 대한 연구는 많으나, TRP 채널의 subfamily 중 하나인 TRPC3 채널에 대한 연구는 미비한 실정이다. 그러므로 본 연구에서, mROS가 가려움증을 유도한다면 mROS가 유도한 가려움증과 TRPC3 채널 사이의 기능적 연관성을 확인하고 TRPC3 채널의 활성 억제가 가려움증을 완화시킬 수 있는지를 검증하고자 하였다.

세포 내 미토콘드리아 전자전달계 복합체 III를 억제하여 mROS의 과잉 생성을 유도하는 것으로 알려져 있는 Antimycin A (AA)를 생쥐 뺨에 피내 주사하여 가려움에 의한 긁기 행동을 유발할 수 있었고, 이러한 긁기 행동이 MitoTEMPO (mROS 제거제) 및 Pyr10 (TRPC3 억제제)에 의해 현저히 완화됨을 확인하였다. AA에 의해 증가된 mROS는 작은 크기의 삼차신경절 단일신경세포에서 활동전위와 내향전류를 발생시켰으며 이 역시 MitoTEMPO 및 Pyr10에 의해 억제되었다. HC-030031 (TRPA1 억제제) 또는 AMG-9810 (TRPV1 억제제) 피내 주사 시, AA에 의해 유도된 긁기 행동이 대조군과 비교하여 차이가 없었으며, TRPA1 KO 및 TRPV1 KO 생쥐에서 보인 긁기 행동도 대조군과의 차이가 없었을 뿐만 아니라, 이들 세포의 내향전류에서도 차이가 없음을 확인하여, mROS에 의해 유도된 가려움증에 TRPC3 채널이 관여함을 알 수 있었다. 더욱이, 작은 크기의 삼차신경절 단일신경세포에서 단일세포 역전사 중합효소 연쇄반응 기술 (scRT-PCR)을 수행한 결과, TRPC3는 기존에 알려진 가려움과 관련된 매개체 및 수용체들과 함께 발현되어 있음을 확인함으로써 TRPC3 채널의 가려움증 매개의 가능성을 제시할 수 있었다. 또한, 건조한 피부 유래 만성 가려움증 모델의 만성 가려움증에서도 mROS 증가 및 TRPC3가 관여함을 조직학적, 행동학적으로 확인하였다.

요약하면, 이 연구는 미토콘드리아 기능 장애로 인한 mROS 증가가 피부의 가려움증을 유발하며, 국지적으로 mROS 증가를 보인 피부건조에서 유래된 만성 가려움증이 TRPC3 채널을 통해 매개된다는 것을 입증하였다. 그러나, mROS가 어떻게 TRPC3를 매개하여 가려움을 유발하는지에 대한 추가적 연구가 필요하다. 이 연구는 TRPC3를 표적으로 작용하는 억제제가 미토콘드리아 기능 이상 및 mROS 증가로 인한 만성 가려움증을 억제하고 치료할 수 있을 것이라는 새로운 가능성을 확인하였다는 점에서 의미가 있다.

주요어: 미토콘드리아, 활성산소종, TRPC3, 가려움증, 피부건조, 삼차신경절
신경세포

학번: 2019-36369